Hyperphosphorylation of JNK-interacting Protein 1, a Protein Associated with Alzheimer Disease*⑤

Chiara D'Ambrosio‡§, Simona Arena‡§, Gabriella Fulcoli‡§, Meir H. Scheinfeld¶, Dawang Zhou¶, Luciano D'Adamio¶‖, and Andrea Scaloni‡**

The c-Jun N-terminal kinase (JNK) group of mitogen-activated protein (MAP) kinases are activated by pleiotropic signals including environmental stresses, growth factors, and hormones. JNK-interacting protein 1 (JIP1) is a scaffold protein that assembles and facilitates the activation of the mixed lineage kinase-dependent JNK module and also establishes an interaction with β-amyloid precursor protein that has been partially characterized. Here we show that, similarly to other proteins involved in various neurological diseases, JIP1 becomes hyperphosphorylated following activation of stress-activated and MAP kinases. By immobilized metal affinity chromatography and a combined microcapillary LC/MALDI-TOF/ESI-ion trap mass spectrometry approach, we identified 35 sites of mitotic phosphorylation within JIP1, among which eight were present within (Ser/Thr)-Pro sequence. This motif is modified by various kinases in aggregates of the microtubule-associated protein tau, which generates typical intraneuronal lesions occurring in Alzheimer disease. Most of the post-translational modifications found were located within the JNK, MAP kinase kinase, and RAC-α Ser/Thr protein kinase binding regions; no modifications occurred in protein Src homology 3 and phosphotyrosine interaction domains, which are essential for binding to kinesin, β-amyloid precursor protein, and MAP kinase kinase kinase. Protein phosphorylation is known to affect stability and protein-protein interactions. Thus, the findings that JIP1 is extensively phosphorylated after activation of stress-activated and MAP kinases indicate that these signaling pathways might modulate JIP1 signaling by regulating its stability and association with some, but not all, interacting proteins. *Molecular & Cellular Proteomics 5:97–113, 2006.*

Alzheimer disease (AD),[1] the most common senile dementia, is characterized by amyloid plaques, vascular amyloid, neurofibrillary tangles (NFTs), and progressive neurodegeneration. Amyloid plaques are mainly composed of Aβ peptides (Aβ40 and Aβ42), which are derived from processing of the ubiquitous type I transmembrane β-amyloid precursor protein (APP) by various secretases (1–4). A pathogenic role for APP processing in AD has been ascertained by the finding that mutations in APP (5) and presenilins (6–9), key components of the γ-secretase, cause AD autosomal dominant familial forms. In AD, APP is first cleaved at the plasma membrane by β-secretase (10) releasing the APPβ ectodomain extracellularly or into intracellular compartments, whereas its C-terminal fragment of 99 amino acids (C99) remains membrane-bound. Then C99 is cleaved by γ-secretase, generating amyloidogenic Aβ peptides and an intracellular product named APP intracellular domain (AID) (11–13). In the non-amyloidogenic proteolytic pathway, APP is first processed by α-secretase in the Aβ peptide sequence leading to the production of APPα and a membrane-bound C-terminal fragment of 83 amino acids (C83). Then C83 is cleaved by γ-secretase into P3 and AID fragments. Although Aβ peptide is implicated in the pathogenesis of AD, AID mediates most of the APP signaling functions. In fact, the AID fragment is able to activate expression of various genes in combination with its binding partner Fe65 (12) or repress it (14, 15). Indeed it has been shown that upon overexpression of APP, Fe65 and Tip60, a repressor complex assembled on the KAI-1 promoter is replaced by a complex containing AID, Fe65, and Tip60. All these reports reinforce the role for AID in gene regulation. Moreover, eight potential phosphorylation sites were predicted on APP cytoplasmic domain. A detailed MS analysis of AD and control brains demonstrated that this region became hyperphosphorylated following the disease (16). This modification seems to affect Aβ peptide generation.

Another pathological feature of AD is the presence of intraneuronal lesions known as NFTs. These are generated by hyperphosphorylated aggregates of the microtubule-associated protein tau and coincide with cell death in several neu-

[1] The abbreviations used are: AD, Alzheimer disease; Aβ, amyloid β; APP, β-amyloid precursor protein; AID, APP intracellular domain; IT, ion trap; JNK, c-Jun N-terminal kinase; JIP, JNK-interacting protein; μLC, microcapillary LC; MAP, mitogen-activated protein; NFT, neurofibrillary tangle; ERK, extracellular signal-regulated kinase; Q, quadrupole.

rodegenerative diseases known as tauopathies (17, 18). Mutations in the tau gene have been linked to NFT formation in a number of tauopathies in which no β-amyloid deposits develop (19, 20). However, no tau gene mutations have been found in AD, and the relationship between tau pathology, amyloid deposition, and neuronal degeneration is still not clear (21, 22). Rampant hyperphosphorylation of tau seems to be the key event associated with NFT formation (17, 18). A complete characterization of tau phosphorylation sites in normal and AD brain required a massive analysis by different mass spectrometric methodologies (23–25). Around 30 modified Ser/Thr residues were identified in tau samples from AD brain, among which a dozen are present in (Ser/Thr)-Pro sites. These motifs, similar to those occurring in other disease-related proteins, are subjected to physiological isomerization and dephosphorylation events (controlled by the peptidyl-prolyl *cis/trans* isomerase Pin1 and the phosphatase PP2A, respectively), which regulate protein conformation/function and NFT formation (18, 26, 27). A growing body of evidence suggests that inappropriate activation of the cell cycle, especially mitotic events, may contribute to this abnormal hyperphosphorylation and thereby play an important role in the development of the disease (18, 28–33).

Previously we have identified JNK-interacting protein 1 (JIP1) as an APP-interacting protein (34, 35). JIP1 was initially identified as an inhibitor of JNK activation but was soon shown to be a scaffold protein that bound various components of the JNK cascade including MKK7, mixed lineage kinase, dual leucine zipper kinase, and other upstream kinases (36). The significance of this APP-JIP1 interaction is still unknown. It is tempting to speculate that JIP1-APP interaction could provide the molecular basis for activation of signaling cascades involving mitogen-activated and stress-activated kinases in the brain of AD patients that may ultimately be responsible for tau hyperphosphorylation and NFT formation (37–41). Preliminary site-directed mutagenesis experiments demonstrated that JIP1 is also phosphorylated, and its modification regulates JNK module dynamics and activation (42). In an attempt to define a possible role of JIP1 in hyperphosphorylation events present in AD cases, which are accompanied by activation of various kinases, we studied the phosphorylation of JIP1 in response to activation of MAP and stress-activated kinases. This investigation, based on the massive use of some recent MS approaches developed to study protein phosphorylation, demonstrates that JIP1 is also hyperphosphorylated.

EXPERIMENTAL PROCEDURES

Reagents—Monoclonal anti-APP N-terminal antibody 22C11 was purchased from Chemicon, and anti-α-tubulin DM 1A was obtained from Sigma. Polyclonal anti-APP C-terminal antibody was purchased from Zymed Laboratories. Polyclonal anti-JNK or -phosphorylated JNK, anti-ERK or -phosphorylated ERK, and anti-p38 or -phosphorylated p38 were obtained from Cell Signaling Technology. Anti-FLAG was from Sigma, and anti-phospho-Tyr and anti-phospho-Thr anti-

bodies were from Cell Signaling Technology. Sequencing grade proteolytic enzymes and phosphatases were purchased from Roche Applied Science. Ultrapure HPLC grade solvents were from Baker. All chemical reagents were purchased from Sigma.

Cell Culture and Transfection—HEK293 cells were maintained in Dulbecco's modified Eagle's medium (Invitrogen) supplemented with 10% fetal bovine serum (Biofluids) and penicillin/streptomycin. Cells were transfected with a construct coding for FLAG-tagged JIP1 by using FuGENE 6 (Roche Applied Science) as described previously (35). Cells were untreated (*control*) or treated with anisomycin (10 μg/ml) for 30 min and lysed in lysis buffer (50 mM Tris-HCl, pH 7.4, 70 mM NaCl, 1 mM Na_3VO_4, 1 mM NaF, 1% (v/v) Triton X-100) containing 2 μg/ml aprotinin, 10 μg/ml leupeptin, 1 mM phenylmethylsulfonyl fluoride. Lysates were boiled in SDS sampling buffer and subjected to SDS-PAGE and Western blotting with the indicated antibodies.

Immunoprecipitation and Immunoblotting Analysis—Twenty-four to 48 h following transfection, cells were washed with ice-cold PBS and lysed in lysis buffer containing a protease inhibitor tablet (Roche Applied Science). Lysis was allowed to continue for 10 min on ice, and cells were centrifuged at full speed at 4 °C for 10 min. Some lysate representing the total lysate was removed and boiled with SDS loading buffer containing DTT, whereas the rest was immunoprecipitated for 2 h at 25 °C with a monoclonal antibody directed against the FLAG epitope already bound to agarose beads (Sigma). The beads were washed five times with lysis buffer and boiled with SDS loading buffer with DTT. Immunoprecipitates and total lysates were separated by SDS-PAGE and blotted onto nitrocellulose (Bio-Rad). Membranes were probed with the same antibodies as were used for immunoprecipitation, and horseradish peroxidase-conjugated secondary antibodies were used. Proteins were detected using the Supersignal West Pico chemiluminescence system (Pierce).

In Vivo Orthophosphate Labeling of Cells—HEK293 cells were transfected with the indicated construct. After 24 h, cells were washed three times with phosphate-free Dulbecco's modified Eagle's medium and incubated at 37 °C in the same medium for 30 min. Cells were then incubated in phosphate-free Dulbecco's modified Eagle's medium containing 0.5% dialyzed fetal bovine serum and 1 mCi/ml [γ-^{32}P]ATP orthophosphate (Amersham Biosciences) for 4 h at 37 °C.

Phosphoamino Acid Analysis—Cellular extracts were resolved by SDS-PAGE and transferred to a PVDF membrane; ^{32}P-labeled JIP1 was identified by autoradiography and excised from the membrane. Blotted protein was subjected to vapor-phase hydrolysis with 6 N HCl at 110 °C for 3 h (43). Two-dimensional phosphoamino acid analysis was carried out on thin layer cellulose plates using the Hunter thin layer electrophoresis system (44). The pattern of phosphoamino acids was visualized by exposing the dried cellulose plates to a model Storm-860 PhosphorImager plate (Amersham Biosciences).

μLC-ESI-Q-MS Analysis—Aliquots of protein extracts containing human JIP1 were analyzed by using an API-100 single quadrupole mass spectrometer (PerkinElmer Sciex) equipped with an electrospray source connected to a Phoenix 40 pump (ThermoFinnigan). Protein extracts were separated on a capillary Hypersil-Keystone Aquasil C_4 Kappa column (100 × 0.32 mm, 5 μm) using a linear gradient from 2 to 60% acetonitrile in 0.1% (v/v) formic acid over 80 min at a flow rate of 5 μl/min. Spectra were acquired in the range 200–2000 *m/z* as reported previously (45). Data were analyzed using the BioMultiView 3.1 software provided by the manufacturer. Mass calibration was performed by means of the multiply charged ions from a separate injection of horse heart myoglobin (molecular mass, 16,951.5 Da). Masses are reported as average values.

In Situ Digestion with Proteolytic Enzymes—Samples containing 10–50 μg of total proteins were subjected to electrophoresis under denaturing conditions on 12% polyacrylamide gels (46). Separated bands were visualized by colloidal Coomassie G250 staining. JIP
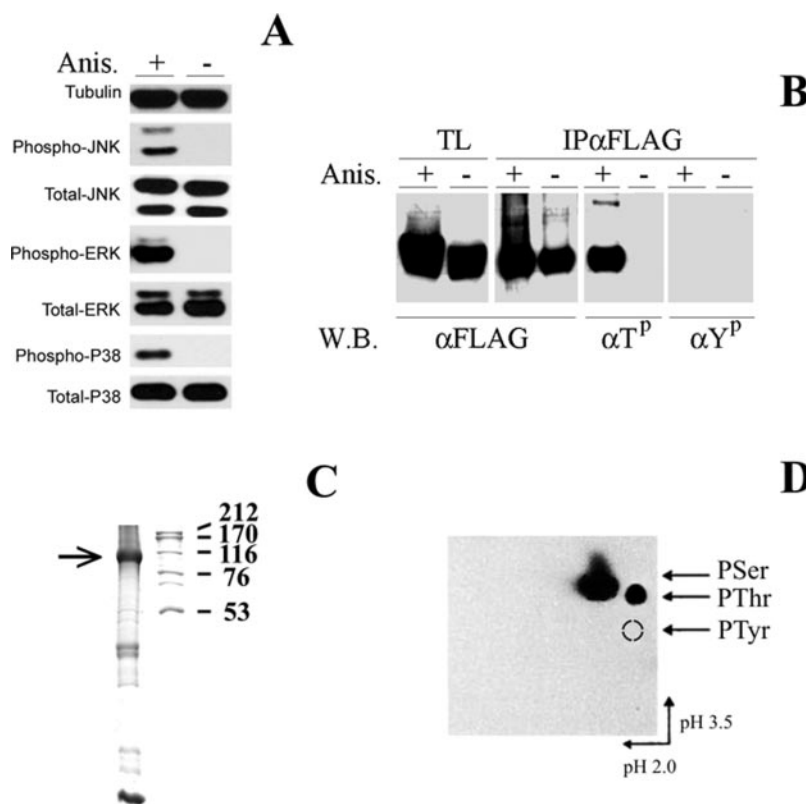
Fɪɢ. 1. **Anisomycin induces stress- and mitogen-activated kinase-mediated phosphorylation of human JIP1 on Ser and Thr residues.** *A*, Western blotting analysis of HEK293 cells transfected with a construct coding for FLAG-tagged JIP1 using anti-α-tubulin, anti-JNK or -phosphorylated JNK, anti-ERK or -phosphorylated ERK, and anti-p38 or -phosphorylated p38 antibodies. Extracts from cells treated (+) or not (−) with anisomycin are shown in comparison. *B*, HEK293 transfected cells before (*TL*) and following (*IPαFLAG*) JIP1 purification with anti-FLAG (*αFLAG*) antibody-agarose beads were assayed by Western blotting with anti-FLAG, anti-phospho-Tyr (*αY*[p]), and anti-phospho-Thr (*αT*[p]) antibodies. *C*, SDS-PAGE analysis of human JIP1 from HEK293 transfected cells following purification with anti-FLAG antibody bound to agarose beads; a Coomassie-stained gel is shown. *D*, qualitative phosphoamino acid analysis of human JIP1. A sample of SDS-PAGE-resolved ^{32}P-labeled JIP1 was electrotransferred onto PVDF membranes, subjected to acid hydrolysis, and analyzed by two-dimensional cellulose thin layer electrophoretic analysis (43, 44). *Anis.*, anisomycin; *W.B.*, Western blot; *IP*, immunoprecipitation; *TL*, total; *PSer*, phospho-Ser, *PThr*, phospho-Thr; *PTyr*, phospho-Tyr.

protein was excised from the gel, triturated, in-gel reduced, *S*-alkylated, and digested either with trypsin or endoprotease AspN, as previously reported (47). Gel particles were extracted with 25 mᴍ NH$_4$HCO$_3$/acetonitrile (1:1 v/v) by sonication and peptide mixtures were concentrated.

Phosphopeptides Enrichment—To isolate phosphopeptides, whole digest aliquots solved in 5% (v/v) acetic acid were loaded on SwellGel Ga^{3+}-chelated discs columns (Pierce) and incubated for 5 min, at 25 °C. Columns were centrifuged at 5000 rpm, for 10 s. Columns were washed with 0.1% (v/v) acetic acid (once), 10% (v/v) acetonitrile in 0.1% (v/v) acetic acid (twice), 50% (v/v) acetonitrile in 0.1% (v/v) acetic acid (twice), and finally with water. Phosphopeptides were initially eluted with 100 mᴍ NH$_4$HCO$_3$, pH 8 and finally with 50% (v/v) acetonitrile in 100 mᴍ NH$_4$HCO$_3$, pH 8. Eluted solutions were mixed and analyzed for phosphopeptides as described below.

μLC Analysis—Aliquots of whole JIP1 digests or phosphopeptide-enriched samples were resolved on a Phoenix 40 LC system (ThermoFinnigan, USA). Peptides were separated on a microbore Jupiter Proteo C12 column (150 × 0.5 mm, 4 μm) using a linear gradient from 2% to 60% of acetonitrile in 0.1% (v/v) trifluoroacetic acid, over 80 min, at flow rate of 20 μl/min. Individual components were collected manually and freeze-dried.
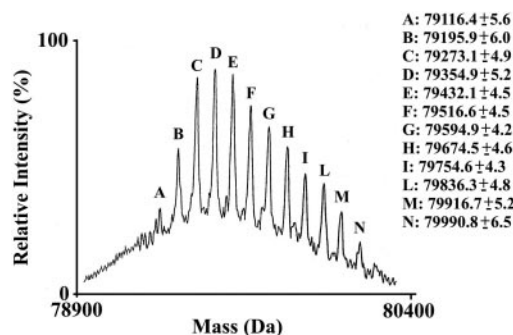
Fɪɢ. 2. **Deconvoluted ESI spectrum of human JIP1.** An aliquot of the protein mixture reported in Fig. 1*C* was analyzed by μLC-ESI-Q-MS as reported under "Experimental Procedures." The spectrum of the most abundant component identified as human JIP1 is shown.

MALDI-TOF-MS Analysis—Aliquots of phosphopeptide mixtures or individual fractions from μLC separation were loaded on the MALDI-TOF instrument target together with 2,5-dihydroxy-benzoic acid (30 mg/ml in 50% (v/v) acetonitrile, 1% (v/v) orthophosphoric acid) as matrix
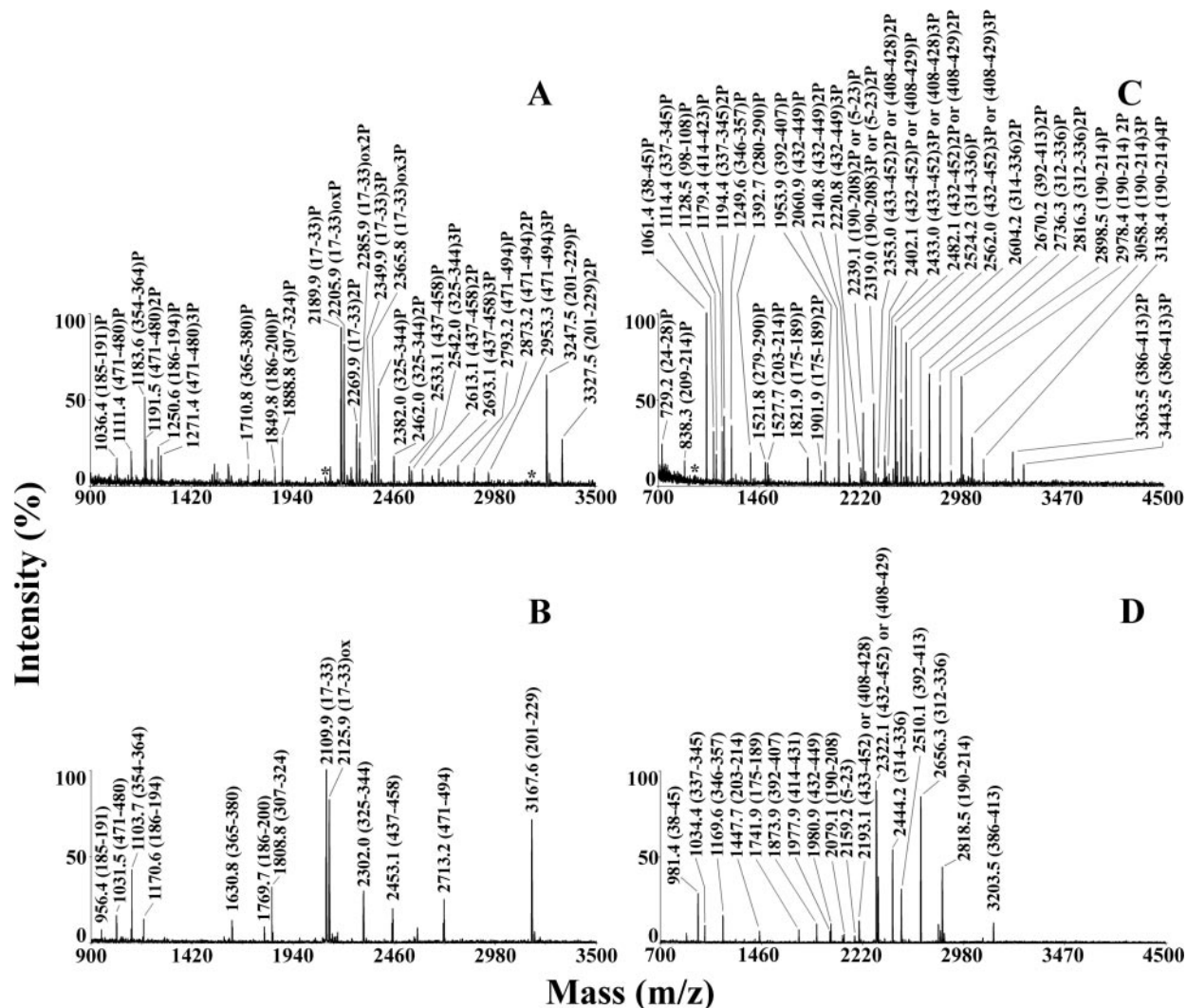
FIG. 3. **MALDI spectrum of human JIP1 phosphopeptides captured by the Ga^{3+} IMAC column before and after treatment with alkaline phosphatase.** The spectrum of the trypsin digest before and after treatment with alkaline phosphatase is shown in *A* and *B,* respectively. The spectrum of the endoprotease AspN digest before and after treatment with alkaline phosphatase is shown in *C* and *D,* respectively. Metastable peaks formed by the loss of HPO$_3^{2-}$ from phosphopeptides (62) are marked with an *asterisk*. Assignment of signals present in *A* and *C* to specific phosphopeptides was performed on the basis of the measured mass, protease specificity, presence of the amino acids susceptible to eventual post-translational modification in the peptide sequence, and signals observed in *B* and *D*.

(48) using the dried droplet technique. Samples were analyzed with a Voyager-DE PRO spectrometer (Applera). Spectra were acquired in positive and negative polarity using the instrument in linear and reflectron mode. Internal or external mass calibration was performed with peptides derived from enzyme autoproteolysis or with molecular mass markers (Applera). Data were elaborated using the DataExplorer 5.1 software (Applera). Masses are reported as monoisotopic values.

μLC-ESI-IT-MS-MS Analysis—Aliquots of whole JIP1 digests or phosphopeptide-enriched samples were analyzed by using a LCQ Deca Xp Plus mass spectrometer (ThermoFinnigan) equipped with an electrospray source connected to a Phoenix 40 pump (ThermoFinnigan). Phosphopeptides were separated on a capillary Hypersil-Keystone Aquasil C$_{18}$ Kappa column (100 × 0.32 mm, 5 μm) using a linear gradient from 2 to 60% acetonitrile in 0.1% (v/v) formic acid over 80 min at a flow rate of 5 μl/min. Spectra were acquired in the range 200–2000 *m/z*. The mass spectrometer was set up to automatically acquire a full MS scan followed by three MS^2 spectra of the

three most abundant ions in the MS spectrum. Spectra were acquired using a dynamic exclusion of 3 min with a mass width of ±2.0 *m/z*. Data were elaborated using the BioWorks 3.1 software provided by the manufacturer. Masses are reported as monoisotopic values.

Alkaline Phosphatase Treatment—Phosphopeptides were dephosphorylated by mixing 3 μl of each sample solved in 50 mM NH$_4$HCO$_3$, pH 8.5, with 2 units of shrimp alkaline phosphatase (Roche Applied Science) solved in 2 μl of 50 mM NH$_4$HCO$_3$. Reaction mixtures were incubated for 60 min at 37 °C followed by addition of 1 μl of 10% (v/v) formic acid. In the case of whole digests, peptide mixtures were desalted on ZipTip C$_{18}$ pipette tips (Millipore) before MALDI-TOF-MS analysis.

Phosphopeptides Subdigestion—Phosphopeptides solved in 5 μl of 50 mM NH$_4$HCO$_3$, pH 8, were subdigested with 30 ng of endoprotease AspN, chymotrypsin, trypsin, or carboxypeptidase A. Reaction mixtures were incubated for 360 min at 37 °C followed by addition of 1 μl of 10% (v/v) formic acid. Digests were directly analyzed by
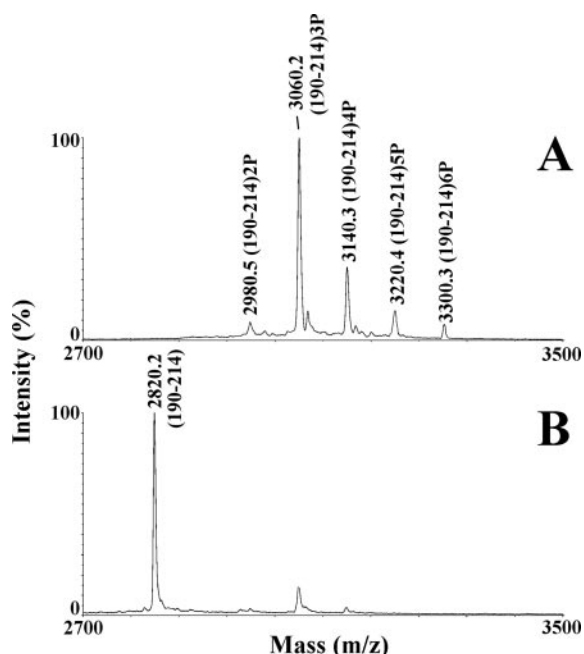
FIG. 4. **Linear MALDI spectrum of a highly phosphorylated peptides present in human JIP1 endoprotease AspN digest captured by Ga³⁺ IMAC column and purified by μLC.** The spectrum of the phosphopeptides present in fraction 25 before and after treatment with alkaline phosphatase is shown in *A* and *B*, respectively. Signals corresponding to peptides (190–214)P5 and (190–214)P6 were not visible in Fig. 3*C*. Masses are reported as average values.

MALDI-TOF-MS.

Data Analysis—Observed MALDI-TOF mass values were assigned to JIP1 phosphopeptides/peptides using the GPMAW 4.23 software (Lighthouse Data). This software generated a mass/fragment database output based on JIP sequence, protease selectivity, nature of the amino acid susceptible to eventual post-translational modification, and molecular mass of the modifying groups. Mass values were matched to protein regions using a 0.02% mass tolerance value. Sequest software allowed automated identification of JIP1 phosphopeptides/peptides using μLC-ESI-IT-MS-MS data (49, 50). This software was run against an indexed database containing human JIP1 and protease sequences by using Met oxidation and Ser/Thr phosphorylation as differential modifications. Values of 2.5 and 1.0 *m/z* were used as mass tolerance for parent and fragment ions, respectively. Candidates with a Sequest Xcorr value >2 were further evaluated by visual inspection of MS² spectra. GPMAW 4.23 software was also used to confirm peptide identification by tandem mass spectrometry data.

Sequence Analysis—A computer-assisted prediction of phosphorylation sites occurring in human JIP1 sequence was obtained by NetPhosK 1.0, NetPhos 2.0, KinasePhos, and GPS software (51–54). Analysis was performed on the FLAG-tagged JIP1 construct coding sequence using program default parameters. Protein domain prediction was performed by the Prosite program (55) using default parameters.

RESULTS

Anisomycin Induces JIP1 Phosphorylation on Ser and Thr Residues—HEK293 cells were transfected with a construct coding for FLAG-tagged JIP1 (35). Twenty-four hours after transfection, cells were treated with anisomycin and then

lysed. To determine whether anisomycin treatment activated stress- and mitogen-activated kinases, lysates were analyzed for phosphorylation of p38, JNK, and ERK. In fact, phosphorylation of these proteins activates their kinase activity. As shown in Fig. 1*A*, anisomycin induced phosphorylation of all the kinases tested, while the total amounts of these proteins were not changed as compared with untreated controls.

Having determined that this experimental condition activated MAP and stress-activated kinases, we purified transfected JIP1 with an anti-FLAG antibody bound to agarose beads. Western blot with an anti-FLAG antibody showed that treated and untreated cells expressed equivalent levels of JIP1; this protein was efficiently immunoprecipitated from both samples (Fig. 1*B*). Moreover immunoblotting with an anti-phospho-Tyr and an anti-phospho-Thr antibody revealed that anisomycin treatment induced phosphorylation of JIP1 on Thr but not Tyr residues. As expected, a Coomassie-stained SDS-PAGE gel of purified JIP1 revealed an abundant protein component with a molecular mass of almost 90 kDa, although polypeptide species presenting lower molecular masses were also detected (Fig. 1*C*). The qualitative nature of JIP1 phosphorylated residues was directly ascertained by phosphoamino acid analysis (43, 44). A sample of ³²P-labeled JIP1 was resolved by SDS-PAGE, electrotransferred onto PVDF membranes, and subjected to acid hydrolysis. Two-dimensional cellulose thin layer electrophoretic analysis definitively demonstrated the occurrence of phospho-Ser and phospho-Thr in JIP1 hydrolysates together with the absence of phospho-Tyr (Fig. 1*D*). To determine the extent to which cellular kinases phosphorylated JIP1 *in vivo*, the molecular mass of the intact protein was determined by μLC-ESI-Q-MS measurements. The spectrum showed a heterogeneous distribution of protein molecular masses, each differing by 80 Da (Fig. 2). The mass difference with respect to the non-phosphorylated protein (theoretical average mass, 78,432.4 Da) and the range of the mass distribution suggested that each mole of JIP1 was modified with 8–19 mol of phosphate. However, the presence of additional phosphate groups at low stoichiometry could not be ruled out as the spectrum was rather noisy. In fact, mass spectra of multiply phosphorylated proteins are inherently noisy relative to non-phosphorylated ones as the signal is being distributed across multiple forms, and metal ion adducts can occur. All these data underlined a reduced estimation of JIP1 phosphorylation (42).

Assignment of Phosphorylation Sites in JIP1—To locate phosphorylation sites in the JIP1 sequence, protein was excised from the gel, alkylated, and digested either with trypsin or endoprotease AspN; small digest aliquots were also treated with alkaline phosphatase (56, 57). MALDI-TOF-MS spectra were obtained and compared, revealing the disappearance of peaks in untreated samples and concomitant appearance of new peaks at masses differing by multiples of −80 Da in treated samples. Thus, four and five phosphorylated peptides could have been identified from whole JIP1

TABLE I

Phosphopeptides present in JIP1 tryptic digest and eluted from the Ga^{3+} IMAC column

Phosphopeptides were identified by a combined approach based on MALDI-TOF-MS analysis of individual fractions from μLC separation and μLC-ESI-IT-MS-MS analysis (see Supplemental Material 1). Masses are reported as monoisotopic values.

MH$^+$ (m/z)	Peptide	Putative phosphorylation sites	HPLC fraction analyzed by MALDI-TOF-MS	Charge in ESI-IT-MS	Identified phosphorylation site
698.3	(195–200)P	195, 196, 197		1, 2	197
908.4	(186–191)P	187		1	187
1036.4	(185–191)P	187	3	2	187
1060.7	(230–238)P	231, 232, 233, 235	1		
1111.4	(471–480)P	471, 472, 473, 476	5	1	
1183.6	(354–364)P	355	7, 8	2	355
1191.5	(471–480)P2	471, 472, 473, 476	4, 5		
1216.6	(230–239)P	231, 232, 233, 235	1	2	235
1250.6	(186–194)P	187, 193	14–17	2, 3	193
1271.4	(471–480)P3	471, 472, 473, 476	4, 5		
1330.6	(186–194)P2	187, 193	19, 20		187, 193
1378.7	(185–194)P	187, 193	18		
1393.5	(460–470)P	466, 469	27		
1439.7	(368–380)P	368, 369, 371, 372, 375, 378		1	
1458.7	(185–194)P2	187, 193	18		187, 193
1498.8	(173–185)P	173, 176, 181		2, 3	181
1521.5	(459–470)P	466, 469	33		
1519.6	(189–200)P2	193, 195, 196, 197		2	
1599.7	(189–200)P3	193, 195, 196, 197		2	
1679.5	(189–200)P4	193, 195, 196, 197		2, 3	193, 195, 196, 197
1710.8	(365–380)P	368, 369, 371, 372, 375, 378	12	1	
1849.8	(186–200)P	187, 193, 195, 196, 197	13		
1888.8	(307–324)P	308, 310, 311, 320, 321	23	2	311
2091.1	(345–364)P	355	26, 27		355
2189.9	(17–33)P[a]	19, 20, 25	33–35	2	20
2200.0	(139–159)P	143, 147, 152, 155	1, 2	2	152 or 155
2269.9	(17–33)P2[a]	19, 20, 25	33–35		
2349.9	(17–33)P3	19, 20, 25	33, 34		19, 20, 25
2382.0	(325–344)P	328, 330, 340, 341	28–31	3, 4	341
2462.0	(325–344)P2	328, 330, 340, 341	27–31		
2533.1	(437–458)P	444, 447, 448, 457	26, 27	3	448
2542.0	(325–344)P3	328, 330, 340, 341	27, 28		
2613.1	(437–458)P2	444, 447, 448, 457	26, 27	3	444, 448
2622.1	(325–344)P4	328, 330, 340, 341	27, 28		328, 330, 340, 341
2643.2	(13–33)P[a]	19, 20, 25	37	3	20
2693.1	(437–458)P3	444, 447, 448, 457	26, 27		
2723.2	(13–33)P2[a]	19, 20, 25	37		
2741.2	(437–459)P2	444, 447, 448, 457	25		
2793.2	(471–494)P	471, 472, 473, 476, 481, 492	39–41	3	
2795.4	(354–380)P	355, 366, 368, 369, 372, 375, 378	30, 31	2, 3	
2803.2	(13–33)P3[a]	19, 20, 25	37	2, 3, 4	19, 20, 25
2873.2	(471–494)P2	471, 472, 473, 476, 481, 492	39		
2875.4	(354–380)P2	355, 366, 369, 372, 375, 378	29, 30	3	
2953.3	(471–494)P3	471, 472, 473, 476, 481, 492	39		
2955.4	(354–380)P3	355, 366, 369, 372, 375, 378	29	3	
3036.4	(469–494)P	469, 471, 472, 473, 476, 492	39–41	3	
3116.4	(469–494)P2	469, 471, 472, 473, 476, 492	39		
3196.4	(469–494)P3	469, 471, 472, 473, 476, 492	39		
3247.5	(201–229)P	201, 205, 214, 226, 227	27–32	3, 4	205
3276.4	(469–494)P4	469, 471, 472, 473, 476, 492	39		
3289.5	(325–353)P	328, 330, 340, 341	33, 34	3, 4	341
3327.5	(201–229)P2	201, 205, 214, 226, 227	27–31	3, 4	205, 214
3369.5	(325–353)P2	328, 330, 340, 341	32, 33	3	340, 341
3546.4	(87–117)P[a]	100, 103		3	100 or 103
3449.5	(325–353)P3	328, 330, 340, 341	32		
3605.8	(275–306)P	278, 284, 296, 297, 303, 305	35, 36	2	284

TABLE I— *continued*

MH$^+$ (*m/z*)	Peptide	Putative phosphorylation sites	HPLC fraction analyzed by MALDI-TOF-MS	Charge in ESI-IT-MS	Identified phosphorylation site
3691.7	(34–63)P	36, 40, 50, 53, 59	40–43	2	40
3926.8	(195–229)P2	195, 196, 197, 201, 205, 214, 226, 227	28–31	4	
4006.8	(195–229)P3	195, 196, 197, 201, 205, 214, 226, 227	28–31	4	
4086.8	(195–229)P4	195, 196, 197, 201, 205, 214, 226, 227	28–31		
4166.8	(195–229)P5	195, 196, 197, 201, 205, 214, 226, 227	28		
4171.8	(307–344)P[a]	308, 311, 320, 321, 328, 330, 340, 341	31–33	3, 4	341
4251.8	(307–344)P2[a]	308, 311, 320, 321, 328, 330, 340, 341	31–33	4	340, 341
4331.8	(307–344)P3[a]	308, 311, 320, 321, 328, 330, 340, 341	30–32		
4411.8	(307–344)P4[a]	308, 311, 320, 321, 328, 330, 340, 341	30, 31		
4727.3	(34–72)P	36, 40, 50, 53, 59, 67	43	4, 5	
4964.4	(195–239)P	195, 196, 197, 201, 205, 214, 226, 227, 231, 232, 235	29		
5044.4	(195–239)P2	195, 196, 197, 201, 205, 214, 226, 227, 231, 232, 235	29, 30		
5079.3	(307–353)P[a]	308, 311, 320, 321, 328, 330, 340, 341	33, 34	3, 4, 5	
5124.4	(195–239)P3	195, 196, 197, 201, 205, 214, 226, 227, 231, 232, 235	29, 30		
5159.3	(307–353)P2[a]	308, 311, 320, 321, 328, 330, 340, 341	33, 34		
5204.4	(195–239)P4	195, 196, 197, 201, 205, 214, 226, 227, 231, 232, 235	29		
5239.3	(307–353)P3[a]	308, 311, 320, 321, 328, 330, 340, 341	33, 34		
5284.4	(195–239)P5	195, 196, 197, 201, 205, 214, 226, 227, 231, 232, 235	29		
5319.3	(307–353)P4[a]	308, 311, 320, 321, 328, 330, 340, 341	33		
5617.6	(87–138)P	100, 103, 130, 137	44	5	100 or 103

[a] Peptides that also occurred as oxidized species.

trypsin and endoprotease AspN digests, respectively (data not shown). These numbers were far fewer than the minimum of 19 suggested by the molecular mass distribution of phosphorylated JIP1.

Because the ionization of phosphopeptides might be suppressed by the presence of large amounts of non-phosphorylated peptides in non-fractionated mixtures (58), both digests were enriched for phosphopeptides by IMAC resin (59–61). The MALDI spectrum of the peptides from trypsin and endoprotease AspN digestion eluted from an IMAC column is shown in Fig. 3, *A* and *C*, respectively. In contrast to previous reports (62), a reduced number of poor satellite signals associated with metastable decomposition of phosphorylated peptides was observed. To identify phosphopeptides, we treated an aliquot of each IMAC fraction with alkaline phosphatase and compared the MALDI spectra taken before and after treatment (57). The spectra of the treated samples were greatly simplified as a result of the collapse of multiply phosphorylated peptides into a single non-phosphorylated peak (Fig. 3, *B* and *D*). Thus, assignment of signals to specific phosphorylated peptides was achieved on the basis of the measured mass, JIP1 sequence, protease selectivity, and nature of the amino acid susceptible to eventual post-translational modification. This analysis demonstrated that most of the signals observed in the spectrum of untreated digests were associated to mono-, di-, tri-, and tetraphosphorylated peptides, thus confirming the high efficiency of the adopted

IMAC procedure in selectively enriching phosphopeptides.

However, because the ionization of highly phosphorylated species might be suppressed by the presence of large amounts of poorly phosphorylated peptides in non-fractionated mixtures, IMAC eluates were also resolved by μLC, and the resulting fractions were analyzed by MALDI-TOF-MS in linear and reflectron modality as well as in negative and positive polarity (63). As an example, Fig. 4*A* shows the spectrum of fraction 25 from the JIP1 endoprotease AspN digest acquired in positive linear mode. In addition to di- to tetraphosphorylated forms of peptide 190–214 (already observed in Fig. 3*C*), mass spectrometric analysis revealed the concomitant occurrence of the penta- and hexaphosphorylated peptide species as also confirmed following digestion with alkaline phosphatase (Fig. 4*B*). Table I summarizes all phosphorylated peptides identified in the trypsin digest; their identity was confirmed following MALDI-TOF-MS analysis of their alkaline phosphatase digests. Peptides deriving from aspecific hydrolysis at Trp-188 and Phe-480 were also detected. Similarly Table II reports all phosphorylated peptides identified in the endoprotease AspN digest. All these results highlighted the importance of μLC fractionation for detection of highly phosphorylated peptides. The eventual loss of small hydrophilic phosphopeptides from JIP1 digests during IMAC enrichment was also evaluated (62, 64). However, MALDI-TOF analysis of both digests after purification on graphite powder microcolumns according to the improved procedure described by

TABLE II

Phosphopeptides present in JIP1 endoprotease AspN digest and eluted from the Ga^{3+} IMAC column

Phosphopeptides were identified by a combined approach based on MALDI-TOF-MS analysis of individual fractions from μLC separation and μLC-ESI-IT-MS-MS analysis (see Supplemental Material 2). Masses are reported as monoisotopic values.

MH$^+$ (m/z)	Peptide	Putative phosphorylation sites	HPLC fraction analyzed by MALDI-TOF-MS	Charge in ESI-IT-MS	Identified phosphorylation site
729.2	(24–28)P	25		1	25
838.3	(209–214)P	214		1	214
840.3	(446–452)P	447, 448		1	448
920.3	(446–452)P2	447, 448	5	1	447, 448
969.3	(445–452)P	447, 448		1	448
1061.4	(38–45)P	40		1	40
1066.4	(405–413)P	407, 409, 411	12	2	411
1114.4	(337–345)P	340, 341	3, 4	1, 2	341
1128.5	(98–108)P	100, 103		1	
1146.4	(405–413)P2	407, 409, 411	12	1	
1179.4	(414–423)P	418, 420, 421	3	1	421
1194.4	(337–345)P2	340, 341	3	1, 2	340, 341
1226.4	(405–413)P3	407, 409, 411	12	1	407, 409, 411
1249.6	(346–357)P	355	24	2	355
1314.6	(358–369)P	366, 368, 369	6, 7	2	369
1392.7	(280–290)P	284		2	284
1394.6	(358–369)P2	366, 368, 369	6, 7	2	
1469.7	(190–202)P	193, 195, 196, 197, 201	3	2, 3	
1521.8	(279–290)P	284		2	284
1527.7	(203–214)P	205, 214	24	2	
1549.7	(190–202 2P	193, 195, 196, 197, 201	3	2	
1607.7	(203–214 2P	205, 214	22	2, 3	205, 214
1660.8	(432–445)P	444	21	2	444
1821.9	(175–189)P	176, 181, 187	23, 24	2, 3	187
1894.0	(8–23)P	19, 20		2	
1901.9	(175–189)P2	176, 181, 187	22		
1953.9	(392–407)P	395, 404, 407	32	2, 3	407
2057.8	(414–431)P	418, 420, 421, 425	8	1	421
2060.9	(432–449)P	444, 447, 448	24		
2140.8	(432–449)P2	444, 447, 448	22, 23	2	447, 448
2159.1	(190–208)P	193, 195, 196, 197, 201, 205	11, 13, 14		
2220.8	(432–449)P3	444, 447, 448	22, 23		444, 447, 448
2239.1	(190–208)P2	193, 195, 196, 197, 201, 205	6–8	2, 3, 4	
2239.1	(5–23)P[a]	19, 20	26	2, 3	20
2260.0	(291–311)P	296, 297, 303, 305, 308, 310, 311	29		
2273.0	(433–452)P	444, 447, 448	23	2	
2273.1	(408–428)P	409, 411, 418, 420, 421, 425	17, 18		
2306.3	(272–290)P	278, 284	25		
2319.0	(190–208)P3	193, 195, 196, 197, 201, 205	3–7	2, 3, 4	
2319.0	(5–23)P2[a]	19, 20	26		19, 20
2353.0	(433–452)P2	444, 447, 448	23		
2353.0	(408–428)P2	409, 411, 418, 420, 421, 425	17		
2377.9	(90–110ox2)P	100, 103	38		
2399.1	(190–208)P4	193, 195, 196, 197, 201, 205	3–6	3	
2402.1	(432–452)P	444, 447, 448	22, 23		
2402.1	(408–429)P	409, 411, 418, 420, 421, 425	18		
2416.2	(2–21)P	19, 20	28		
2433.0	(433–452)P3	444, 447, 448	22, 23		444, 447, 448
2433.0	(408–428)P3	409, 411, 418, 420, 421, 425	17		
2465.2	(346–369)P	355, 366, 368, 369	27	3	355
2479.1	(190–208)P5	193, 195, 196, 197, 201, 205	3		
2482.1	(432–452)P2	444, 447, 448	23		444, 447, 448
2482.1	(408–429)P2	409, 411, 418, 420, 421, 425	19		
2496.0	(2–21)P2	19, 20	28		19, 20
2524.2	(314–336)P	320, 321, 328, 330	27, 28	2, 3	330
2539.1	(424–445)P	425, 444	25		

TABLE II— *continued*

MH$^+$ (m/z)	Peptide	Putative phosphorylation sites	HPLC fraction analyzed by MALDI-TOF-MS	Charge in ESI-IT-MS	Identified phosphorylation site
2562.0	(432–452)P3	444, 447, 448	23, 24		444, 447, 448
2562.0	(408–429)P3	409, 411, 418, 420, 421, 425	19		
2567.3	(453–474)P	457, 466, 469, 471, 472, 473	36, 37		
2604.2	(314–336)P2	320, 321, 328, 330	26, 27	2, 3	328, 330
2647.2	(386–407)P	395, 404, 407		3	407
2647.3	(453–474)P2	457, 466, 469, 471, 472, 473	36, 37		
2670.2	(392–413)P2	395, 404, 407, 409, 411	31–35	3	
2727.3	(453–474)P3	457, 466, 469, 471, 472, 473	36, 37		
2736.3	(312–336)P	320, 321, 328, 330	28, 29	2, 3	330
2750.2	(392–413)P3	395, 404, 407, 409, 411	31, 32		
2774.2	(430–452)P2	444, 447, 448	23		
2807.3	(453–474)P4	457, 466, 469, 471, 472, 473	36, 37		
2816.3	(312–336)P2	320, 321, 328, 330	28	2, 3	
2821.4	(343–369)P	355, 366, 368, 369	33		
2854.2	(430–452)P3	444, 447, 448	23		444, 447, 448
2898.5	(190–214)P	193, 195, 196, 197, 201, 205, 214	26–28	3, 4, 5	
2901.4	(343–369)P2	355, 366, 368, 369	33		
2949.4	(5–28)P2[a]	19, 20, 25	35, 36		
2978.4	(190–214)P2	193, 195, 196, 197, 201, 205, 214	25–27	2 ,3 ,4, 5	
2981.4	(343–369)P3	355, 366, 368, 369	33		
3029.4	(5–28)P3[a]	19, 20, 25	34, 35		19, 20, 25
3046.4	(102–129)P	103	14, 15		103
3058.4	(190–214)P3	193, 195, 196, 197, 201, 205, 214	25–27	2, 3, 4	
3138.4	(190–214)P4	193, 195, 196, 197, 201, 205, 214	24–26	3, 4	
3202.6	(346–376)P	355, 366, 368, 369, 371, 372, 375	31, 32	3	
3218.4	(190–214)P5	193, 195, 196, 197, 201, 205, 214	24, 25		
3243.6	(234–264)P[a]	235, 240, 241, 243, 262	23, 24	3, 4, 5	235
3282.6	(346–376)P2	355, 366, 368, 369, 371, 372, 375	30–32		
3283.5	(386–413)P	382, 395, 404, 407, 409, 411	46		
3298.4	(190–214)P6	193, 195, 196, 197, 201, 205, 214	25		
3362.6	(346–376)P3	355, 366, 368, 369, 371, 372, 375	29–31		
3363.5	(386–413)P2	382, 395, 404, 407, 409, 411	45		
3443.5	(386–413)P3	382, 395, 404, 407, 409, 411	45		
3633.7	(280–311)P2	284, 296, 297, 303, 305, 308, 310, 311			
3860.9	(228–264)P	231, 232, 233, 235, 240, 241, 243, 262	23, 24		
4040.0	(114–153)P	131, 137, 143, 147, 152	3		
4127.0	(234–271)P[a]	235, 240, 241, 243, 262	26, 27	4	
4155.0	(113–153)P	131, 137, 143, 147, 152	3, 4		
4270.0	(112–153)P	131, 137, 143, 147, 152	3–5		
4389.1	(370–407)P	371, 372, 375, 378, 382, 395, 404, 407	42–60		
4640.1	(294–336)P[a]	308, 311, 320, 321, 328, 330	33		
4643.1	(109–153)P	131, 137, 143, 147, 152	6, 7	5	
4720.1	(294–336)P2[a]	308, 311, 320, 321, 328, 330	33		
4758.1	(108–153)P	131, 137, 143, 147, 152	7		
4800.1	(294–336)P3	308, 311, 320, 321, 328, 330	32		
4897.2	(291–336)P[a]	308, 311, 320, 321, 328, 330	31–35	3	
4977.2	(291–336)P2[a]	308, 311, 320, 321, 328, 330	32, 33	3	
5057.2	(291–336)P3	308, 311, 320, 321, 328, 330	32, 33		
5328.4	(102–153)P	103, 131, 137, 143, 147, 152	9–16	3, 4, 5, 6	103
5408.1	(102–153)P2	103, 131, 137, 143, 147, 152	10, 11		
5672.4	(98–153)P	100, 103, 131, 137, 143, 147, 152	15, 16	4, 6	103
5752.4	(98–153)P2	100, 103, 131, 137, 143, 147, 152	15	3, 4, 5	
6182.0	(453–504)P[a]	457, 466, 469, 471, 472, 473, 476, 481, 492	42, 43	5, 6	
6262.0	(453–504)P2	457, 466, 469, 471, 472, 473, 476, 481, 492	42, 43		
6334.1	(234–290)P	235, 240, 243, 262, 278, 284	34–40		
6342.0	(453–504)P3	457, 466, 469, 471, 472, 473, 476, 481, 492	42, 43		
6414.1	(234–290)P2	235, 240, 243, 262, 278, 284	33		
6422.0	(453–504)P4	457, 466, 469, 471, 472, 473, 476, 481, 492	42, 43		

[a] Peptides that also occurred as oxidized species.
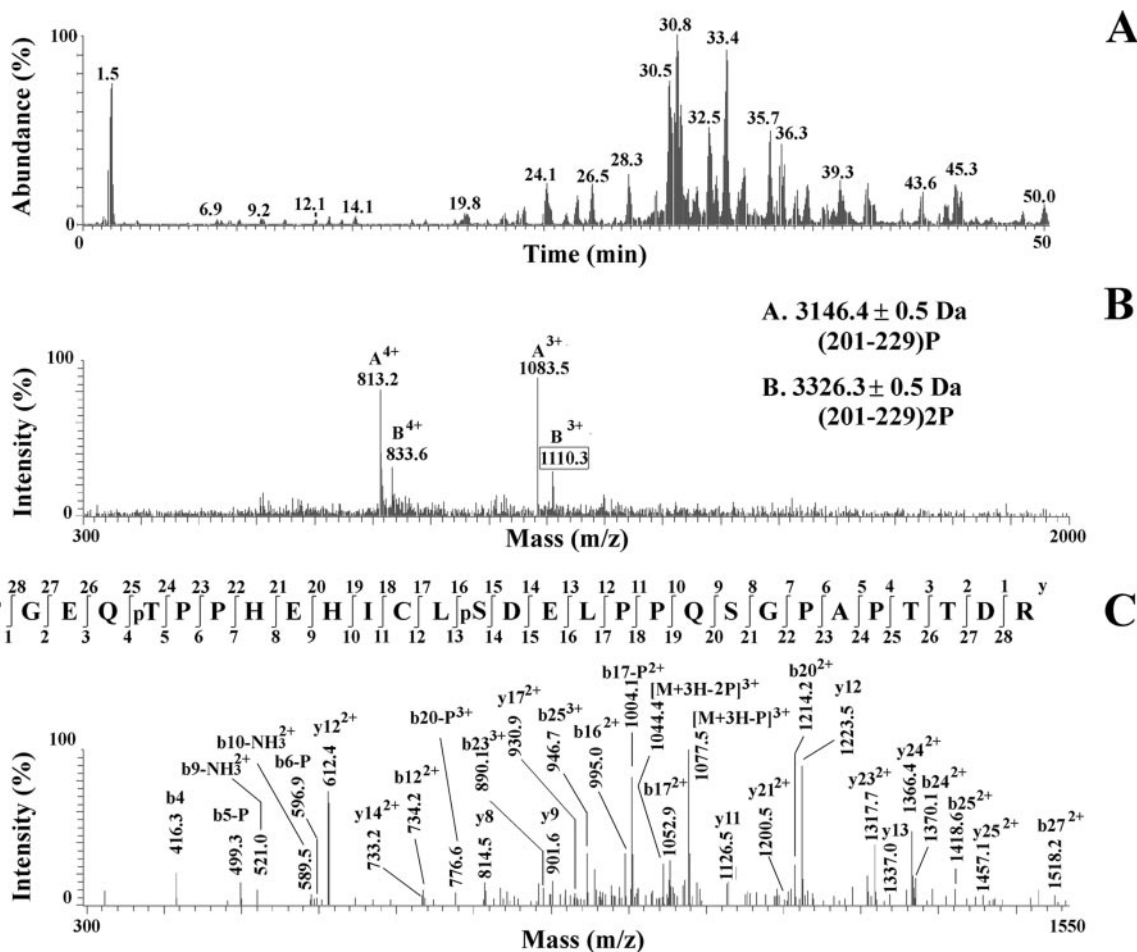
FIG. 5. **µLC-ESI-IT-MS-MS analysis of phosphopeptides captured by the Ga³⁺ IMAC column in human JIP1 tryptic digest.** *A* shows the total ion chromatogram of the tryptic digest separated on a capillary reversed phase HPLC column and acquired on an ion trap mass spectrometer as described under "Experimental Procedures." *B* shows the positive ion spectrum of the peak at 30.8 min containing triply and quadruply charged ions associated to peptides (201–229)P and (201–229)P2, which gave MS^2 spectra with abundant ions resulting from the neutral loss of 32.7 *m/z* ($H_3PO_4/3$) and 24.5 *m/z* ($H_3PO_4/4$), respectively. Tandem mass spectrometry analysis of the triply charged ion at 1110.3 *m/z* (indicated as the *boxed* species) is shown in *C*. This spectrum allowed direct assignment of Thr(P)-205 and Ser(P)-214. For simplicity, the abundant ions resulting from the single or double neutral loss of 32.7 *m/z* ($H_3PO_4/3$) from the triply charged ion are indicated with [M + 3H − P]$^{3+}$ and [M + 3H − 2P]$^{3+}$, respectively.

Larsen *et al.* (64) did not allow detection of phosphopeptides other than those already reported in Tables I and II.

Phosphopeptides identified by MALDI-TOF analysis were also analyzed by tandem mass spectrometry to confirm their identity and determine the site(s) of phosphorylation (56, 58). Thus, IMAC eluates of trypsin and endoprotease AspN digests were subjected to µLC-ESI-IT-MS-MS analysis (49, 50, 65). Phosphopeptides were easily recognized by examination of their positive mode MS^2 spectra for an abundant ion resulting from the neutral loss of 98 *m/z* (H_3PO_4) for a singly charged, 49 *m/z* ($H_3PO_4/2$) for a doubly charged, 32.7 *m/z* ($H_3PO_4/3$) for a triply charged, or 24.5 *m/z* ($H_3PO_4/4$) for a quadruply charged ion for each phospho-Ser or phospho-Thr in the peptide (33, 50, 51, 53). Most of the peaks observed in chromatograms were associated to phosphorylated peptides, confirming the high efficiency of the adopted IMAC procedure

in selectively enriching phosphorylated species (Fig. 5*A*). In most cases, fragmentation data allowed assigning the exact sites of modification as clearly shown in the case of the tryptic peptide (201–229)P2 (Fig. 5, *B* and *C*). In total, sequencing data were obtained for 40 of 68 tryptic phosphopeptides already detected by MALDI-TOF-MS analysis (Table I and Supplemental Material 1); in addition, eight new phosphopeptides were identified. Similarly sequencing data were obtained for 54 of 103 phosphopeptides from the endoprotease AspN digest already detected by MALDI-TOF-MS analysis (Table II and Supplemental Material 2) with 12 new phosphopeptides identified. Tables I and II show all identified phosphorylated species together with the assignment of 29 phosphorylation sites. In fact, this combined approach allowed demonstration that phosphorylation occurred at Ser-19, Ser-20, Ser-25, Ser-40, Thr-103, Ser-181, Ser-187, Ser-193, Ser-195, Ser-196,

Ser-197, Thr-205, Thr-214, Ser-235, Thr-284, Ser-311, Ser-328, Ser-330, Ser-340, Ser-341, Ser-355, Ser-369, Ser-407, Ser-409, Thr-411, Ser-421, Ser-444, Ser-447, and Thr-448. Moreover a series of MS^2 spectra recorded during μLC-ESI-IT-MS-MS analysis of tryptic and endoprotease AspN digests demonstrated that JIP1 is acetylated at the N terminus (data not shown).

To complete assignment of phosphorylation sites and confirm data derived by MALDI-TOF-MS and μLC-ESI-IT-MS-MS analysis, selected peptide fractions from μLC purification of trypsin and endoprotease AspN digests (see Tables I and II) were subjected to further digestion with various proteases and then subjected to MALDI-TOF-MS analysis. Table III summarizes all phosphorylated peptides identified in subdigestion mixtures; their identities were also ascertained following alkaline phosphatase treatment and further MALDI-TOF-MS analysis (data not shown). This approach allowed demonstration that phosphorylation occurred at Ser-152, Ser-366, Ser-469, Ser-471, Ser-472, and Ser-473. Thus, all data reported in Fig. 3 and Tables I, II, and III were consistent with each other and allowed the identifing of all phosphorylation sites present *in vivo* in human JIP1.

Trypsin and endoprotease AspN digests not subjected to IMAC enrichment were also analyzed by μLC-ESI-IT-MS-MS procedures. As reported in the case of MALDI-TOF analysis, the majority of the most intense ions in chromatogram were assigned to non-phosphorylated peptides (data not shown). A combination of data deriving from MALDI-TOF-MS and μLC-ESI-IT-MS-MS analyses allowed the obtaining of complete overall sequence coverage for JIP1 protein, also demonstrating that a partial modification occurred on all assigned phosphorylation sites. In fact, all peptides detected as phosphorylated species were also present as non-phosphorylated counterparts. This result was in perfect agreement with the extent of phosphorylation on intact protein revealed by ESI-MS measurement (Fig. 2).

A theoretical prediction of phosphorylation sites occurring in human JIP1 sequence was achieved by four independent computer-assisted methodologies (51–54). This approach was chosen to consider the maximum number of kinases (eventually not included by a single program). Analysis revealed that human JIP1 sequence contains 118 putative modification sites recognized by a broad number of kinases; 20, 28, 38, and 32 sites were simultaneously ascertained by four, three, two, and one programs, respectively. Predicted phosphorylated Ser, Thr, and Tyr residues are reported in Fig. 6. In contrast, our mass spectrometry-based investigation showed the absence of Tyr modification, demonstrating the occurrence of 35 phosphorylation sites, among which eight were present in (Ser/Thr)-Pro motifs. All residues characterized as phosphorylated by previous site-directed mutagenesis studies (42) were confirmed by our investigation; in addition, 24 novel phosphorylation sites were identified, among which one (Ser-214) was not predicted by computer-assisted analysis.

Most post-translational modifications were located within the JNK, MAP kinase kinase, and RAC-α Ser/Thr protein kinase binding regions of JIP1 sequence not affecting protein Src homology 3, APP, and phospho-Tyr interaction domains (34–36, 42, 55).

DISCUSSION

Progression through different phases of the cell cycle is controlled by highly regulated sequential activation and inactivation of cyclin-dependent kinases (28). Cyclin-dependent kinases belong to the family of Pro-directed kinases and also include ERKs, JNKs, and glycogen synthase kinase-3β, which phosphorylate almost exclusively on (Ser/Thr)-Pro motifs. Therefore, phosphorylation of (Ser/Thr)-Pro motifs is the central mechanism governing progression through different phases of the cell cycle. At the G_2-M transition, activation of cyclin B/Cdc2 leads to the phosphorylation of a number of proteins. Many of these phosphoproteins (such as Cdc25, Wee1, Myt1, and RNA polymerase II) are important mitotic regulators and also contain multiple (Ser/Thr)-Pro signatures (18, 66). An intriguing feature common to these proteins is that they are phosphorylated on multiple Ser/Thr residues clustered at the regulatory domain of molecules during mitosis. Phosphorylation on multiple sites is necessary for activation/inactivation of their function in M phase (67, 68). A major mechanism that reverses these phosphorylation events is dephosphorylation by protein phosphatases. In this regard, PP2A is an important enzyme that dephosphorylates the conserved (Ser/Thr)-Pro motifs present in a number of mitotic proteins and plays an essential role in mitotic regulation (27).

Although the etiology of AD is variable, all AD cases exhibit a similar hierarchical and progressive pattern of relentless neuronal death in brain, resulting from disruption of cytoskeleton networks and formation of hallmark NFTs and Aβ peptide plaques. One biochemical hallmark of degenerating neurons is rampant tau hyperphosphorylation on multiple (Ser/Thr)-Pro motifs (17, 23–25). Similarly an abnormal hyperphosphorylation of (Ser/Thr)-Pro sites has been depicted as a distinct feature characterizing neurofilament protein NF-H and vimentin in many neurological diseases (AD, Parkinson disease, and amyotrophic lateral sclerosis) (33, 69), tumor suppressor BARD1 and BRCA2 in breast cancer (32, 70), epidermal growth factor receptor in mammary and squamous carcinomas (31), stathmin in fibroblast transformation (30), retinoid X receptor in apoptosis (29), and heat shock factor I in stress conditions (71). These findings emphasize that a deregulation of the processes controlling a proper protein phosphorylation should determine non-functional hyperphosphorylated species and result in other mitotic events, apoptosis, and ultimately cellular death. Strong support for the role of cell cycle mechanisms in AD comes from the findings that AD neurons contain multiple markers spanning different phases of the cell cycle (72). Furthermore Yang *et al.* (73) demonstrated recently that AD neurons may have synthesized DNA but fail to com-

TABLE III
Assignment of phosphorylation sites in JIP1 by enzymatic subdigestion of phosphopeptides purified from tryptic and endoprotease AspN digests

Fractions from μLC separation (see Tables I and II) were subjected to further treatment with endoprotease AspN, chymotrypsin, trypsin, or carboxypeptidase A. Masses are reported as monoisotopic values.

Tryptic fraction	MH+ (m/z)	Peptide	Putative phosphorylation sites	MH+	Subdigestion products	Identified phosphorylation site
				Da		
1, 2	2200.0	(139–159)P[a]	143, 147, 152, 155	1439.6	(139–153)P	152
26, 27	2533.1	(437–458)P[a]	444, 447, 448, 457	1478.6	(437–449)P	
				1819.7	(437–452)P	
26, 27	2613.1	(437–458)P2[a]	444, 447, 448, 457	1558.6	(437–449)P2	
				1899.7	(437–452)P2	
26, 27	2693.1	(437–458)P3[a]	444, 447, 448, 457	1638.6	(437–449)P3	444, 447, 448
				1979.7	(437–452)P3	
39–41	2793.2	(471–494)P[a]	471, 472, 473, 476, 481, 492	2381.1	475–494	
				2141.9	(471–489)P	
30, 31	2795.4	(354–380)P[b]	355, 366, 368, 369, 372, 375, 378	1454.7	(354–367)P	
				1117.6	357–367	
39	2873.2	(471–494)P2[a]	471, 472, 473, 476, 481, 492	2381.1	475–494	
				2221.9	(471–489)P2	
29, 30	2875.4	(354–380)P2[b]	355, 366, 369, 372, 375, 378	1534.7	(354–367)P2	355, 366
				1197.6	(357–367)P	
39	2953.3	(471–494)P3[a]	471, 472, 473, 476, 481, 492	2381.1	475–494	471, 472, 473
				2301.9	(471–489)P3	
29	2955.4	(354–380)P3[b]	355, 366, 369, 372, 375, 378	1534.7	(354–367)P2	355, 366
				1197.6	(357–367)P	
39–41	3036.4	(469–494)P[a]	469, 471, 472, 473, 476, 492	2381.1	475–494	
				2385.0	(469–489)P	
39	3116.4	(469–494)P2[a]	469, 471, 472, 473, 476, 492	2381.1	475–494	
				2465.0	(469–489)P2	
39	3196.4	(469–494)P3[a]	469, 471, 472, 473, 476, 492	2381.1	475–494	
				2545.0	(469–489)P3	
27–32	3247.5	(201–229)P[a]	201, 205, 214, 226, 227	1527.7	(203–214)P	
				2818.3	(203–227)P	
39	3276.4	(469–494)P4[a]	469, 471, 472, 473, 476, 492	2381.1	475–494	469, 471, 472, 473
				2625.0	(469–489)P4	
27–31	3327.5	(201–229)P2[a]	201, 205, 214, 226, 227	1607.7	(203–214)P2	205, 214
				2898.3	(203–227)P2	

AspN fraction	MH+ (m/z)	Peptide	Putative phosphorylation sites	Mass	Subdigestion products	Identified phosphorylation site
6, 7	1394.6	(358–369)P2[b]	366, 368, 369	1140.6	(358–367)P	366
17	2353.0	(408–428)P2[b]	409, 411, 418, 420, 421, 425	735.3	(408–413)P	
				1179.4	(414–423)P	
18	2402.1	(408–429)P[b]	409, 411, 418, 420, 421, 425	655.3	408–413	
				1179.4	(414–423)P	
17	2433.0	(408–428)P3[b]	409, 411, 418, 420, 421, 425	815.3	(408–413)P2	409, 411
				1179.4	(414–423)P	
19	2482.1	(408–429)P2[b]	409, 411, 418, 420, 421, 425	735.3	(408–413)P	
				1179.4	(414–423)P	
19	2562.1	(408–429)P3[b]	409, 411, 418, 420, 421, 425	815.3	(408–413)P2	409, 411
				1179.4	(414–423)P	
36, 37	2567.3	(453–474)P[c]	457, 466, 469, 471, 472, 473	732.4	453–458	
				860.5	453–459	
				1070.5	460–468	
36, 37	2647.3	(453–474)P2[c]	457, 466, 469, 471, 472, 473	732.4	453–458	
				860.5	453–459	
				1070.5	460–468	

TABLE III— *continued*

AspN fraction	MH$^+$ (m/z)	Peptide	Putative phosphorylation sites	Mass	Subdigestion products	Identified phosphorylation site
31–35	2670.2	(392–413)P2[a]	395, 404, 407, 409, 411	1177.6	392–401	
				1542.7	392–404	
				2068.8	(392–408)P	
				1146.4	(405–413)P2	
36, 37	2727.3	(453–474)P3[c]	457, 466, 469, 471, 472, 473	732.4	453–458	
				860.5	453–459	
				1070.5	460–468	
31, 32	2750.2	(392–413)P3[a]	395, 404, 407, 409, 411	1542.7	392–404	407, 409, 411
				2068.8	(392–408)P	
				1146.4	(405–413)P3	
36, 37	2807.3	(453–474)P4[c]	457, 466, 469, 471, 472, 473	732.4	453–458	469, 471, 472, 473
				860.5	453–459	
				1070.5	460–468	
33	2821.4	(343–369)P[b]	355, 366, 368, 369	1610.8	(353–367)P	
				1117.6	357–367	
26–28	2898.5	(190–214)P[b]	193, 195, 196, 197, 201, 205, 214	1183.6	(190–199)P	
33	2901.4	(343–369)P2[b]	355, 366, 368, 369	1690.8	(353–367)P2	355, 366
				1197.6	(357–367)P	
25–27	2978.4	(190–214)P2[b]	193, 195, 196, 197, 201, 205, 214	1183.6	(190–199)P	
33	2981.4	(343–369)P3[b]	355, 366, 368, 369	1690.8	(353–367)P2	355, 366
				1197.6	(357–367)P	
25–27	3058.4	(190–214)P3[b]	193, 195, 196, 197, 201, 205, 214	1263.6	(190–199)P2	
24–26	3138.4	(190–214)P4[b]	193, 195, 196, 197, 201, 205, 214	1263.6	(190–199)P2	
31, 32	3202.6	(346–376)P[b]	355, 366, 368, 369, 371, 372, 375	1610.8	(353–367)P	
				1117.6	357–367	
24, 25	3218.4	(190–214)P5[b]	193, 195, 196, 197, 201, 205, 214	1343.6	(190–199)P3	
30–32	3282.6	(346–376)P2[b]	355, 366, 368, 369, 371, 372, 375	1690.8	(353–367)P2	355, 366
				1197.6	(357–367)P	
46	3283.5	(386–413)P[a]	382, 395, 404, 407, 409, 411	1870.9	386–401	
				2236.0	386–404	
				2762.2	(386–408)P	
				1066.4	(405–413)P	
25	3298.4	(190–214)P6[b]	193, 195, 196, 197, 201, 205, 214	1423.6	(190–199)P4	193, 195, 196, 197
29–31	3362.6	(346–376)P3[b]	355, 366, 368, 369, 371, 372, 375	1690.8	(353–367)P2	355, 366
				1197.6	(357–367)P	
45	3363.5	(386–413)P2[a]	382, 395, 404, 407, 409, 411	2236.0	386–404	
				2762.2	(386–408)P	
				1146.4	(405–413)P2	
45	3443.5	(386–413)P3[a]	382, 395, 404, 407, 409, 411	1870.9	386–401	407, 409, 411
				2236.0	386–404	
				2762.2	(386–408)P	
				1226.4	(405–413)P3	
3	4040.0	(114–153)P[d]	131, 137, 143, 147, 152	3982.8	(114–152)P	152
				3815.8	114–151	
				3758.8	114–150	
3, 4	4155.0	(113–153)P[d]	131, 137, 143, 147, 152	4097.9	(113–152)P	152
				3930.8	113–151	
3–5	4270.0	(112–153)P[d]	131, 137, 143, 147, 152	4212.9	(112–152)P	152
				4045.8	112–151	
				3988.8	112–150	
9–16	5328.4	(102–153)P[c]	103, 131, 137, 143, 147, 152	2214.8	(102–120)P	103
10, 11	5408.1	(102–153)P2[c]	103, 131, 137, 143, 147, 152	2214.8	(102–120)P	103
				1439.6	(139–153)P	

[a] Treatment with endoprotease AspN.
[b] Treatment with chymotrypsin.
[c] Treatment with trypsin.
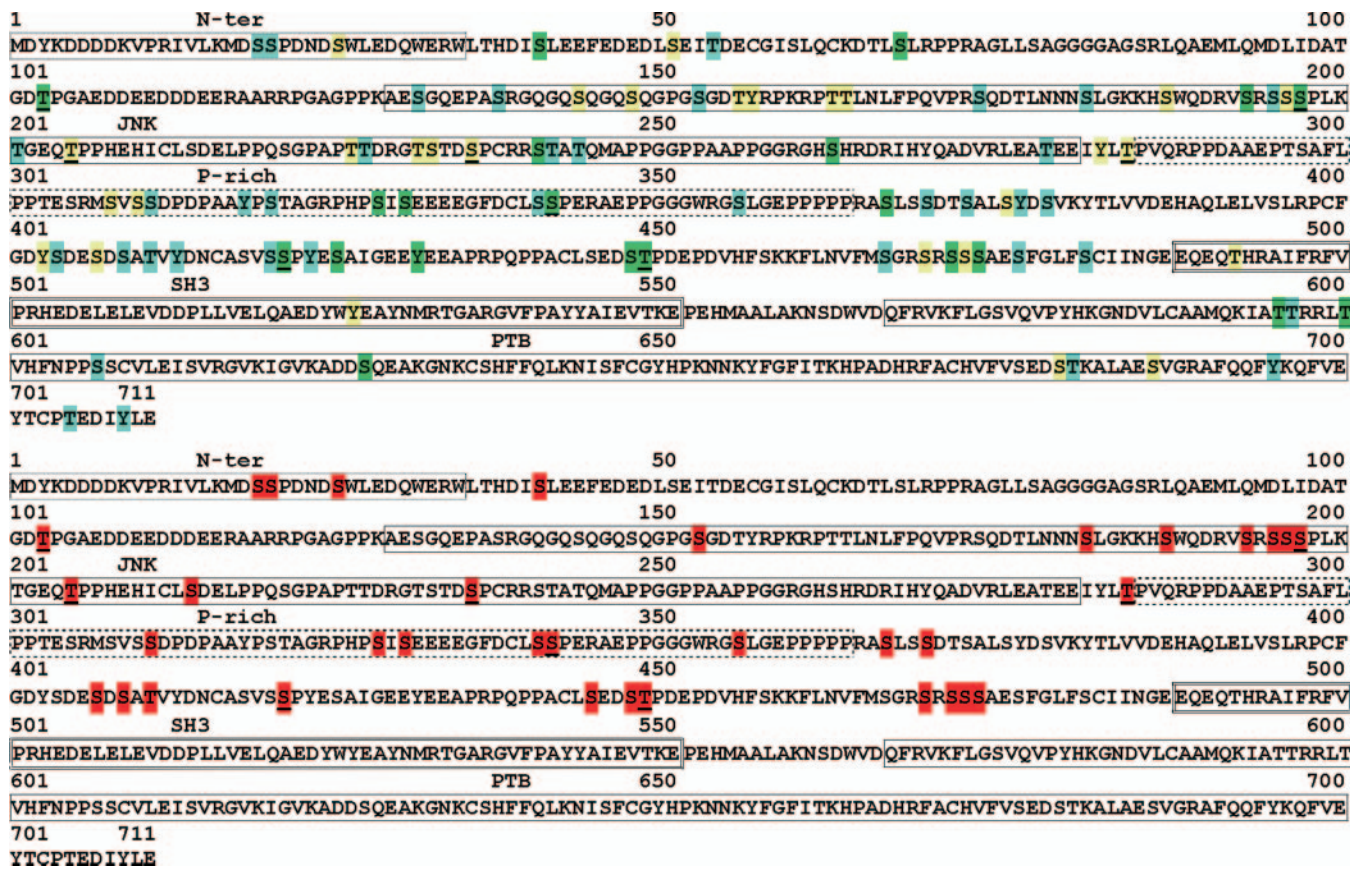[d] Treatment with carboxypeptidase A.

Fig. 6. **Computer-predicted and mass spectrometry-determined phosphorylation sites in human JIP1.** Both panels show the exogenous N-terminal (*N-ter*), JNK interaction, Pro-rich, Src homology 3, and phosphotyrosine interaction domains present in human JIP1 sequence predicted by the Prosite program as regions *boxed* with a different style (55). Theoretical phosphorylation sites calculated according to NetPhosK 1.0, NetPhos 2.0, KinasePhos, and GPS software (51–54) are reported in the *upper panel*. Putative sites recognized by four, three, and two programs are highlighted in *green*, *yellow*, and *light blue*, respectively. Phosphorylation sites determined by site-directed mutagenesis (42) are *underlined*. The *bottom panel* shows phosphorylation sites ascertained by mass spectrometry that are highlighted in *red*.

plete M phase, so that the cells remain tetraploid. Probably the most striking feature common to the normal cell cycle and degenerating neurons of AD brain is that they share many mitotic events especially phosphorylation on certain (Ser/Thr)-Pro motifs in proteins such as tau. However, monoclonal antibodies recognizing independent phosphorylated epitopes in NFTs showed strong immunoreactivity with cells in mitosis but not in interphase in various cell types (18, 74–76). Reciprocally the phosphospecific monoclonal antibody MPM-2 raised against mitotic cells specifically labeled affected neurons with aberrant activation of the mitotic Cdc2 kinase in AD brain but with no immunoreactivity in normal neurons (77, 78). Of significance is the incorporation of mitotic phospho-epitopes into NFTs and their appearance prior to NFT formation in AD brain, suggesting their involvement in early stages of AD pathology. In addition, phosphorylation of APP and production of amyloidogenic fragments from APP are seen in normal mitotic cells (79). Finally there is a tight link between the mitotic mechanism and apoptosis; induction of mitosis in postmitotic neuronal cells leads inevitably to cell death (80, 81). Indeed apoptosis is elevated in hippocampal brain tissue

in AD (82, 83). A closer comparison of normal mitotic cells with AD neurons has revealed not only many similarities but also some striking differences. The similarities are seen in the type of players involved, but the dissimilarities are observed in the timing of their appearance and their subcellular localization. For example, activation of cyclin B/Cdc2 occurs in the cytoplasm and then in the nucleus during normal mitosis, but such activation apparently occurs only in the cytoplasm of AD neurons (84–86). It is suggested that these differences simply would not support normal mitosis and may be important determinants of the degenerative fate of neurons (87).

Because of the central role of phosphorylation in the regulation of cellular processes, much effort has been focused on the development of methodologies for characterizing this protein modification. Nowadays mass spectrometry is the most used analytical technique to study protein phosphorylation (56, 58). This modification is often substoichiometric, and phosphopeptide enrichment procedures are a necessary prerequisite for characterization of hyperphosphorylated proteins by modern MALDI and ESI mass spectrometric methods. As an example, an integrated use of these methodologies re-

cently has allowed assignment of 10 phosphorylation sites in BARD1 tumor suppressor (32), 12 sites in human heat shock factor I (71), 19 sites in mitotic regulator Net1 (62), 33 sites in tau (23–25), and 38 sites in neurofilament protein NF-H (33). In this study, we used an integrated MALDI and ESI mass spectrometric approach to demonstrate that, under experimental conditions mimicking activation of mitogen-activated and stress-activated kinases, a protein able to interact with JNK, APP, and various components of the JNK cascade (34–36), namely JIP1, is *in vivo* hyperphosphorylated. A total number of 35 phosphorylation sites were assigned on its polypeptide sequence, among which eight occurred in (Ser/Thr)-Pro motifs. Accordingly JIP1 can be considered among the most hyperphosphorylated of known proteins so far.

What is the biological function of JIP1 phosphorylation? This post-translational modification can affect protein function in distinct ways. In some cases, phosphorylation targets proteins for ubiquitination and degradation. Important examples are cell cycle proteins (88) and IκB, the inhibitor of the transcription factor NFκB (89). In others cases, phosphorylation generates docking sites for protein-protein interaction. This is the case for some phospho-Tyr residues that can create docking sites for proteins containing Src homology 2 domains (90) or for phospho-Ser/phospho-Thr binding modules, which include 14-3-3 proteins, WW domains, forkhead-associated domains, WD40 repeats, and the Polo-box domains of Polo-like kinases (91). As for JIP1, it is conceivable to postulate that phosphorylation of some residues might affect JIP1 stability and conformation or impact on the association of JIP1 with its various binding partners (34–36, 42). A detailed analysis is required to address the significance of each JIP1 phosphorylation site, and it will be the topic of further investigation by site-directed mutagenesis.

REFERENCES

1. Kang, J., Lemaire, H. G., Unterbeck, A., Salbaum, J. M., Masters, C. L., Grzeschik, K. H., Multhaup, G., Beyreuther, K., and Muller-Hill, B. (1987) The precursor of Alzheimer's disease amyloid A4 protein resembles a cell-surface receptor. *Nature* **325,** 733–736

2. Selkoe, D., and Kopan, R. (2003) Notch and presenilin: regulated intramembrane proteolysis links development and degeneration. *Annu. Rev. Neurosci.* **26,** 565–597

3. Sisodia, S. S., and St George-Hyslop, P. H. (2002) γ-Secretase, Notch, Aβ and Alzheimer's disease: where do the presenilins fit in? *Nat. Rev. Neurosci.* **3,** 281–290

4. Gandy, S. (2005) The role of cerebral amyloid β accumulation in common forms of Alzheimer disease. *J. Clin. Investig.* **115,** 1121–1129

5. Goate, A., Chartier-Harlin, M. C., Mullan, M., Brown, J., Crawford, F., Fidani, L., Giuffra, L., Haynes, A., Irving, N., James, L., Mant, R., Newton, P., Rooke, K., Roques, P., Talbot, C., Pericak-Vance, M., Roses, A., Williamson, R., Rossor, M., Owen, M., and Hardy, J. (1991) Segregation of a missense mutation in the amyloid precursor protein gene with familial Alzheimer's disease. *Nature* **349,** 704–706

6. Sherrington, R., Rogaev, E. I., Liang, Y., Rogaeva, E. A., Levesque, G., Ikeda, M., Chi, H., Lin, C., Li, G., Holman, K., Tsuda, T., Mar, L., Foncin, J.-F., Bruni, A. C., Montesi, M. P., Sorbi, S., Rainero, I., Pinessi, L., Nee, L., I., Chumakov, Pollen, D., Brookes, A., Sanseau, P., Polinsky, R. J., Wasco, W., Da Silva, H. A. R., Haines, J. L., Pericak-Vance, M. A., Tanzi, R. E., Roses, A. D., Fraser P. E., Rommens, J. M., and St George-Hyslop, P. H. (1995) Cloning of a gene bearing missense mutations in early-onset familial Alzheimer's disease. *Nature* **375,** 754–760

7. Levy-Lahad, E., Wasco, W., Poorkaj, P., Romano, D. M., Oshima, J., Pettingell, W. H., Yu, C. E., Jondro, P. D., Schmidt, S. D., Wang, K., Crowley, A. C., Fu, Y.-H., Guenette, S. Y., Galas, D., Nemens, E., Wijsman, E. M., Bird, T. D., Schelleneg, G. D., and Tanzi, R. E. (1995) Candidate gene for the chromosome 1 familial Alzheimer's disease locus. *Science* **269,** 973–977

8. Levy-Lahad, E., Wijsman, E. M., Nemens, E., Anderson, L., Goddard, K. A., Weber, J. L., Bird, T. D., and Schellenberg, G. D. (1995) A familial Alzheimer's disease locus on chromosome 1. *Science* **269,** 970–973

9. Rogaev, E. I., Sherrington, R., Rogaeva, E. A., Levesque, G., Ikeda, M., Liang, Y., Chi, H., Lin, C., Holman, K., Tsuda, T., Mar, L., Sorbi, S., Nacmias, B., Piacentini, S., Amaducci, L., Chumakov, I., Cohen, D., Lannfelt, L., Fraser, P. E., Rommens, J. M., and St George-Hyslop, P. H. (1995) Familial Alzheimer's disease in kindreds with missense mutations in a gene on chromosome 1 related to the Alzheimer's disease type 3 gene. *Nature* **376,** 775–778

10. Vassar, R., Bennett, B. D., Babu-Khan, S., Kahn, S., Mendiaz, E. A., Denis, P., Teplow, D. B., Ross, S., Amarante, P., Loeloff, R., Luo, Y., Fisher, S., Fuller, J., Edenson, S., Lile, J., Jarosinski, M. A., Biere, A. L., Curran, E., Burgess, T., Louis, J. C., Collins, F., Treanor, J., Rogers, G., and Citron, M. (1999) β-Secretase cleavage of Alzheimer's amyloid precursor protein by the transmembrane aspartic protease BACE. *Science* **286,** 735–741

11. Passer, B., Pellegrini, L., Russo, C., Siegel, R. M., Lenardo, M. J., Schettini, G., Bachmann, M., Tabaton, M., and D'Adamio, L. (2000) Generation of an apoptotic intracellular peptide by γ-secretase cleavage of Alzheimer's amyloid β protein precursor. *J. Alzheimer's Dis.* **2,** 289–301

12. Cao, X., and Sudhof, T. C. (2001) A transcriptionally active complex of APP with Fe65 and histone acetyltransferase Tip60. *Science* **293,** 115–120

13. Cupers, P., Orlans, I., Craessaerts, K., Annaert, W., and De Strooper, B. (2001) The amyloid precursor protein (APP)-cytoplasmic fragment generated by γ-secretase is rapidly degraded but distributes partially in a nuclear fraction of neurones in culture. *J. Neurochem.* **78,** 1168–1178

14. Gao, Y., and Pimplikar, S. W. (2001) The γ-secretase-cleaved C-terminal fragment of amyloid precursor protein mediates signaling to the nucleus. *Proc. Natl. Acad. Sci. U. S. A.* **98,** 14979–14984

15. Roncarati, R. Sestan, N., Scheinfeld, M. H., Berechid, B. E., Lopez, P. A., McGlade, J. C., Meucci O., Rakic, P., and D'Adamio, L. (2002) The γ-secretase-generated intracellular domain of beta-amyloid precursor protein binds Numb and inhibits Notch signaling. *Proc. Natl. Acad. Sci. U. S. A.* **99,** 7102–7707

16. Lee, M. S., Kao, S. C., Lemere, C. A., Xia, W., Tseng, H. C., Zhou, Y., Neve, R., Ahlijanian, M. K., and Tsai, L. H. (2003) App processing is regulated by cytoplasmic phosphorylation. *J. Cell Biol.* **163,** 83–95

17. Alonso, A., Zaidi, T., Novak, M., Grundke-Iqbal, I., and Iqbal, K. (2001) Hyperphosphorylation induces self-assembly of tau into tangles of paired helical filaments/straight filaments. *Proc. Natl. Acad. Sci. U. S. A.* **98,** 6923–6928

18. Lu, K. P., Liou, Y., and Vincent, I. (2003) Proline-directed phosphorylation

and isomerization in mitotic regulation and in Alzheimer's disease. *BioEssays* **25,** 174–181

19. Hutton, M. (2001) Missense and splice site mutations in tau associated with FTDP-17: multiple pathogenic mechanisms. *Neurology* **56,** S21-S25

20. Spillantini, M. G., and Goedert, M. (1998) Tau protein pathology in neurodegenerative diseases. *Trends Neurosci.* **21,** 428–433

21. Hardy J. A., and Higgins, G. A. (1992) Alzheimer's disease: the amyloid cascade hypothesis. *Science* **256,** 184–185

22. Taylor, J. P., Hardy, J., and Fischbeck, K. H. (2002) Toxic proteins in neurodegenerative disease. *Science* **296,** 1991–1995

23. Hanger, D. P., Betts, J. C., Loviny, T. L., Blackstock, W. P., and Anderton, B. H. (1998) New phosphorylation sites identified in hyperphosphorylated tau (paired helical filament-tau) from Alzheimer's disease brain using nanoelectrospray mass spectrometry. *J. Neurochem.* **71,** 2465–2476

24. Lund, E. T., McKenna, R., Evans, D. B., Sharma, S. K., and Mathews, W. R. (2001) Characterization of the in vitro phosphorylation of human tau by tau protein kinase II (cdk5/p20) using mass spectrometry. *J. Neurochem.* **76,** 1221–1232

25. Morishima-Kawashima, M., Hasegawa, M., Takio, K., Suzuki, M., Yoshida, H., Titani, K., and Ihara, Y. (1995) Proline-directed and non-proline-directed phosphorylation of PHF-tau. *J. Biol. Chem.* **270,** 823–829

26. Lu, P. J., Wulf, G., Zhou, X. Z., Davies, P., and Lu, K. P. (1999) The prolyl isomerase Pin1 restores the function of Alzheimer-associated phosphorylated tau protein. *Nature* **399,** 784–788

27. Zhou, X. Z., Kops, O., Werner, A., Lu, P. J., Shen, M., Stoller, G., Kullertz, G., Stark, M., Fisher, G., and Lu, K. P. (2000) Pin1-dependent prolyl isomerization regulates dephosphorylation of Cdc25C and tau proteins. *Mol. Cell* **6,** 873–883

28. Nigg, E. A. (2001) Mitotic kinases as regulators of cell division and its checkpoints. *Nat. Rev. Mol. Cell Biol.* **13,** 261–291

29. Adam-Stitah, S., Penna, L., Chambon, P., and Rochette-Egly, C. (1999) Hyperphosphorylation of the retinoid X receptor α by activated JNK. *J. Biol. Chem.* **274,** 18932–18941

30. Lovric, J., Dammeier, S., Kieser, A., Mischak, H., and Kolch, W. (1998) Activated raf induces the hyperphosphorylation of stathmin and the reorganization of the microtubule network. *J. Biol. Chem.* **273,** 22848–22855

31. Boeri Erba, E., Bergatto, E., Cabodi, S., Silengo, L., Tarone, G., Defilippi, P., and Jensen, O. N. (2005) Systematic analysis of the EGF receptor by mass spectrometry reveals stimulation-dependent multisite phosphorylation. **4,** 1107–1121

32. Choudhury, A. D., Xu, H., Modi, A. P., Zhang, W., Ludwig, T., and Baer R. (2005) Hyperphosphorylation of the BARD1 tumor suppressor in mitotic cells. *J. Biol. Chem.* **280,** 24669–24679

33. Jaffe, H., Veeranna, Shetty, K. T., and Pant, H. C. (1998) Characterization of the phosphorylation sites of human high molecular weight neurofilament protein by electrospray ionization tandem mass spectrometry and database searching. *Biochemistry* **37,** 3931–3940

34. Matsuda, S., Yasukawa, T., Homma, Y., Ito, Y., Niikura, T., Hiraki, T., Hirai, S., Ohno, S., Kita, Y., Kawasumi, M., Kouyama, K., Yamamoto, T., Kyriakis, J. M., and Nishimoto, I. (2001) c-Jun N-terminal kinase (JNK)-interacting Protein-1b/islet-brain-1 scaffolds Alzheimer's amyloid precursor protein with JNK. *J. Neurosci.* **21,** 6597–6607

35. Scheinfeld, M. H., Roncarati, R., Vito, P., Lopez, P. A., Abdallah, M., and D'Adamio, L. (2002) Jun NH$_2$-terminal kinase (JNK) interacting protein 1 (JIP1) binds the cytoplasmic domain of the Alzheimer's β-amyloid precursor protein (APP). *J. Biol. Chem.* **277,** 3767–3775

36. Dickens, M., Rogers, J. S., Cavanagh, J., Raitano, A., Xia, Z., Halpern, J. R., Greenberg, M. E., Sawyers, C. L., and Davis, R. J. (1997) A cytoplasmic inhibitor of the JNK signal transduction pathway. *Science* **277,** 693–696

37. Whitmarsh, A. J., Cavanagh, J., Tournier, C., Yasuda, J., and Davis, R. J. (1998) A mammalian scaffold complex that selectively mediates MAP kinase activation. *Science* **281,** 1671–1674

38. Zhu, X., Raina, A. K., Rottkamp, C. A., Aliev, G., Perry, G., Boux, H., and Smith, M. A. (2001) Activation and redistribution of c-jun N-terminal kinase/stress activated protein kinase in degenerating neurons in Alzheimer's disease. *J. Neurochem.* **76,** 435–441

39. Shoji, M., Iwakami, N., Takeuchi, S., Waragai, M., Suzuki, M., Kanazawa, I., Lippa, C. F., Ono, S., and Okazawa, H. (2000) JNK activation is associated with intracellular β-amyloid accumulation. *Brain Res. Mol. Brain Res.* **85,** 221–233

40. Reynolds, C. H., Utton, M. A., Gibb, G. M., Yates, A., and Anderton, B. H. (1997) Stress-activated protein kinase/c-jun N-terminal kinase phosphorylates tau protein. *J. Neurochem.* **68,** 1736–1744

41. Zhu, X., Castellani, R. J., Takeda, A., Nunomura, A., Atwood, C. S., Perry, G., and Smith, M. A. (2001) Differential activation of neuronal ERK, JNK/SAPK and p38 in Alzheimer disease: the 'two hit' hypothesis. *Mech. Ageing Dev.* **123,** 39–46

42. Nihalani, D., Wong, H. N., and Holzman, L. B. (2003) Recruitment of JNK to JIP1 and JNK-dependent JIP1 phosphorylation regulates JNK module dynamics and activation. *J. Biol. Chem.* **278,** 28694–28702

43. Duclos, B., Marcandier, S., and Cozzone, A. (1991) Chemical properties and separation of phosphoamino acids by thin-layer chromatography and/or electrophoresis. *Methods Enzymol.* **201,** 10–21

44. Kamps, M. (1991) Determination of phosphoamino acid composition by acid hydrolysis of protein blotted to Immobilon. *Methods Enzymol.* **201,** 21–27

45. Cecconi, I., Scaloni, A., Rastelli, G., Moroni, M., Vilardo, P. G., Costantino, L., Cappiello, M., Garland, D., Carper, D., Petrash, J. M., Del Corso, A., and Mura, U. (2002) Oxidative modification of aldose reductase induced by copper ion. Definition of the metal-protein interaction mechanism. *J. Biol. Chem.* **277,** 42017–42027

46. Laemmli, U. (1970) Cleavage of structural proteins during the assembly of the head of bacteriophage T4. *Nature* **227,** 680–685

47. Allegrini, S., Scaloni, A., Ferrara, L., Pesi, R., Pinna, P., Sgarrella, F., Camici, M., Eriksson, S., and Tozzi, M. G. (2001) Bovine cytosolic 5′-nucleotidase acts through the formation of an aspartate 52-phosphoenzyme intermediate. *J. Biol. Chem.* **276,** 33526–33532

48. Kjellstrom, S., and Jensen, O. N. (2004) Phosphoric acid as a matrix additive for MALDI MS analysis of phosphopeptides and phosphoproteins. *Anal. Chem.* **76,** 5109–5117

49. MacCoss, M. J., McDonald, W. H., Saraf, A., Sadygov, R., Clark, J. M., Tasto, J. J., Gould, K. L., Wolters, D., Washburn, M., Weiss, A., Clark, J. I., and Yates, J. R., III (2002) Shotgun identification of protein modifications from protein complexes and lens tissue. *Proc. Natl. Acad. Sci. U. S. A.* **99,** 7900–7905

50. Beausoleil, S. A., Jedrychowski, M., Schwartz, D., Elias, J. E., Villen, J., Li, J., Cohn, M. A., Cantley, L. C., and Gygi, S. P. (2004) Large-scale characterization of HeLa cell nuclear phosphoproteins. *Proc. Natl. Acad. Sci. U. S. A.* **101,** 12130–12135

51. Blom, N., Gammeltoft, S., and Brunak, S. (1999) Sequence- and structure-based prediction of eukaryotic protein phosphorylation sites. *J. Mol. Biol.* **294,** 1351–1362

52. Blom, N., Sicheritz-Ponten, T., Gupta, R., Gammeltoft, S., and Brunak, S. (2004) Prediction of post-translational glycosylation and phosphorylation of proteins from the amino acid sequence. *Proteomics* **4,** 1633–1649

53. Huang, H. D., Lee, T. Z., Tzeng, S. W., and Horng, J. T. (2005) KinasePhos: a web tool for identifying protein kinase-specific phosphorylation sites. *Nucleic Acids Res.* **33,** W226–W229

54. Xue, Y., Zhou, F., Zhu, M., Ahmed, K., Chen, G., and Yao, X. (2005) GPS: a comprehensive www server for phosphorylation sites prediction. *Nucleic Acids Res.* **33,** W184–W187

55. Hulo, N., Sigrist, C. J. A., Le Saux, V., Langendijk-Genevaux, P. S., Bordoli, L., Gattiker, A., De Castro, E., Bucher, P., and Bairoch, A. (2004) Recent improvements to the PROSITE database. *Nucleic Acids Res.* **32,** D134–D137

56. McLachlin, D. T., and Chait, B. T. (2001) Analysis of phosphorylated proteins and peptides by mass spectrometry. *Curr. Opin. Chem. Biol.* **5,** 591–602

57. Larsen, M. R., Sorensen, G. L., Fey, S. J., Larsen, P. M., and Roepstorff, P. (2001) Phospho-proteomics: evaluation of the use of enzymatic dephosphorylation and differential mass spectrometric peptide mass mapping for site specific phosphorylation assignment in proteins separated by gel electrophoresis. *Proteomics* **1,** 223–238

58. Mann, M., Ong, S. E., Gronborg, M., Steen, H., Jensen, O. N., and Pandey, A. (2002) Analysis of protein phosphorylation using mass spectrometry: deciphering the phosphoproteome. *Trends Biotechnol.* **20,** 261–268

59. Posewitz, M. C., and Tempst, P. (1999) Immobilized gallium(III) affinity chromatography of phosphopeptides. *Anal. Chem.* **71,** 2883–2892

60. Li, S. H., and Dass, C. (1999) Iron(III)-immobilized metal ion affinity chromatography and mass spectrometry for the purification and characterization of synthetic phosphopeptides. *Anal. Biochem.* **270,** 9–14

61. Nuhse, T. S., Stensballe, A., Jensen, O. N., and Peck, S. C. (2003) Large-scale analysis of *in vivo* phosphorylated membrane proteins by immobilized metal ion affinity chromatography and mass spectrometry. *Mol. Cell. Proteomics* **2,** 1234–1243

62. Loughrey Chen, S., Huddleston, M. J., Shou, W., Deshaies, R. J., Annan, R. S., and Carr, S. A. (2002) Mass spectrometry-based methods for phosphorylation site mapping of hyperphosphorylated proteins applied to Net1, a regulator of exit from mitosis in yeast. *Mol. Cell. Proteomics* **1,** 186–196

63. Ma, Y., Lu, Y., Zeng, H., Ron, D., Mo, W., and Neubert, T. A. (2001) Characterization of phosphopeptides from protein digests using matrix-assisted laser desorption/ionization time-of-flight mass spectrometry and nanoelectrospray quadrupole time-of-flight mass spectrometry. *Rapid Commun. Mass Spectrom.* **15,** 1693–1700

64. Larsen, M. R., Graham, M. E., Robinson, P. J., and Roepstorff, P. (2004) Improved detection of hydrophilic phosphopeptides using graphite powder microcolumns and mass spectrometry. Evidence for in vivo doubly phosphorylated dynamin I and dynamin III. *Mol. Cell. Proteomics* **3,** 456–465

65. Ficarro, S. B., McCleland, M. L., Stukenberg, P. T., Burke, D. J., Ross, M. M., Shabanowitz, J., Hunt, D. F., and White, F. M. (2002) Phosphoproteome analysis by mass spectrometry and its application to *Saccharomyces cerevisiae*. *Nat. Biotechnol.* **20,** 301–305

66. Yaffe, M. B., Schutkowski, M., Shen, M., Zhou, X. Z., Stukenberg, P. T., Rahfeld, J. U., Xu, J., Kuang, J., Kirschner, M. W., Fischer, G., Cantley, L. C., and Lu K. P. (1997) Sequence-specific and phosphorylation-dependent proline isomerization: a potential mitotic regulatory mechanism. *Science* **278,** 1957–1960

67. Matsumoto-Taniura, N., Pirollet, F., Monroe, R., Gerace, L., and Westendorf, J. M. (1996) Identification of novel M phase phosphoproteins by expression cloning. *Mol. Biol. Cell* **7,** 1455–1469

68. Izumi, T., and Maller, J. L. (1993) Elimination of cdc2 phosphorylation sites in the cdc25 phosphatase blocks initiation of M-phase. *Mol. Biol. Cell* **4,** 1337–1350

69. Eriksson, J. E., He, T., Trejo-Skalli, A. V., Harmala-Braskèn, A., Hellman, J., Chou, Y. H., and Goldman, R. D. (2004) Specific in vivo phosphorylation sites determine the assembly dynamics of vimentin intermediate filaments. *J. Cell Sci.* **117,** 919–932

70. Lin, H. R., Ting, N. S., Qin, J., and Lee, W. H. (2003) M phase-specific phosphorylation of BRCA2 by Polo-like kinase 1 correlates with the dissociation of the BRCA2-P/CAF complex. *J. Biol. Chem.* **278,** 35979–35987

71. Guettouche, T., Boellmann, F., Lane, W. S., and Voellmy, R. (2005) Analysis of phosphorylation of human heat shock factor 1 in cells experiencing a stress. *BMC Biochem.* **6,** 4–14

72. Nagy, Z., Esiri, M. M., and Smith, A. D. (1998) The cell division cycle and the pathophysiology of Alzheimer's disease. *Neuroscience* **87,** 731–739

73. Yang, D., Geldmacher, S., and Herrup, K. (2001) DNA replication precedes neuronal cell death in Alzheimer's disease. *J. Neurosci.* **21,** 2661–2668

74. Illenberger, S., Zheng-Fischhofer, Q., Preuss, U., Stamer, K., Baumann, K., Trinczek, B., Biernat, J., Godemann, R., Mandelkow, E. M., and Mandelkow, E. (1998) The endogenous and cell cycle-dependent phosphorylation of tau protein in living cells: implications for Alzheimer's disease.

Mol. Biol. Cell **9,** 1495–1512

75. Preuss, U., and Mandelkow, E. M. (1998) Mitotic phosphorylation of tau protein in neuronal cell lines resembles phosphorylation in Alzheimer's disease. *Eur. J. Cell Biol.* **76,** 176–184

76. Dranovsky, A., Vincent, I., Gregori, L., Schwarzman, A., Colflesh, D., Enghild, J., Strittmatter, W., Davies, P., and Goldgaber, D. (2001) Cdc2 phosphorylation of nucleolin demarcates mitotic stages and Alzheimer's disease pathology. *Neurobiol. Aging* **22,** 517–528

77. Vincent, I., Zheng, J. H., Dickson, D. W., Kress, Y., and Davies, P. (1998) Mitotic phosphoepitopes precede paired helical filaments in Alzheimer's disease. *Neurobiol. Aging* **19,** 287–296

78. Kondratick, C. M., and Vandre, D. D. (1996) Alzheimer's disease neurofibrillary tangles contain mitosis-specific phosphoepitopes. *J. Neurochem.* **67,** 2405–2416

79. Suzuki, T., Oishi, M., Marshak, D. R., Czernik, A. J., Nairn, A. C., and Greengard, P. (1994) Cell cycle-dependent regulation of the phosphorylation and metabolism of the Alzheimer amyloid precursor protein. *EMBO J.* **13,** 1114–1122

80. King, K. L., and Cidlowski, J. A. (1995) Cell cycle and apoptosis: common pathways to life and death. *J. Cell. Biochem.* **58,** 175–180

81. Park, D. S., Farinelli, S. E., and Greene, L. A. (1996) Inhibitors of cyclin-dependent kinases promote survival of post-mitotic neuronally differentiated PC12 cells and sympathetic neurons. *J. Biol. Chem.* **271,** 8161–8169

82. Smale, G., Nichols, N. R., Brady, D. R., Finch, C. E., and Horton, W. E., Jr. (1995) Evidence for apoptotic cell death in Alzheimer's disease. *Exp. Neurol.* **133,** 225–230

83. Li, W. P., Chan, W. Y., Lai, H. W., and Yew, D. T. (1997) Terminal dUTP nick end labelling (TUNEL) positive cells in the different regions of the brain in normal aging and Alzheimer patients. *J. Mol. Neurosci.* **8,** 75–82

84. Ding, X. L., Husseman, J., Tomashevski, A., Nochlin, D., Jin, L. W., and Vincent, I. (2000) The cell cycle Cdc25A tyrosine phosphatase is activated in degenerating postmitotic neurons in Alzheimer's disease. *Am. J. Pathol.* **157,** 1983–1990

85. Vincent, I., Bu, B., Tomashevski, A., Husseman, J., Nochlin, D., and Jin, L. W. (2001) Constitutive Cdc25B activity in adult brain neurons with M phase-type alterations in Alzheimer neurodegeneration. *Neuroscience* **105,** 639–650

86. Tomashevski, A., Husseman, J., Jin, L. W., Nochlin, D., and Vincent, I. (2001) Constitutive Wee1 activity in adult brain neurons with M phase-type alterations in Alzheimer neurodegeneration. *J. Alzheimer's Dis.* **3,** 195–207

87. Vincent, I. (2000) Cycling to the finish. *Neurobiol. Aging* **21,** 757–760

88. Bloom, J., and Pagano, M. (2004) To be or not to be ubiquitinated? *Cell Cycle* **3,** 138–140

89. Ravid, T., and Hochstrasser, M. (2004) NF-κB signaling: flipping the switch with polyubiquitin chains. *Curr. Biol.* **14,** R898–R900

90. Pawson, T. (2004) Specificity in signal transduction: from phosphotyrosine-SH2 domain interactions to complex cellular systems. *Cell* **116,** 191–203

91. Yaffe, M. B., and Smerdon, S. J. (2004) The use of in vitro peptide-library screens in the analysis of phosphoserine/threonine-binding domain structure and function. *Annu. Rev. Biophys. Biomol. Struct.* **33,** 225–244